TURUN
YLIOPISTO
Matemaattis-luonnontieteellinen
tiedekunta

The validation of antibodies with genetic strategy: PP2A inhibitors CIP2A, PME-1 and SET in human triple-negative breast cancer cell lines

Suvi Rajaniemi

Physiology and Genetics
Master's thesis
Credits: 30 ECTS

10.11.2025
Turku

The originality of this thesis has been checked in accordance with the University of Turku quality assurance system using the Turnitin Originality Check service.

Master's thesis

Subject: Physiology and Genetics, Biology
Author: Suvi Rajaniemi
Title: The validation of antibodies with genetic strategy: PP2A inhibitors CIP2A, PME-1 and SET in human triple-negative breast cancer cell lines
Supervisors: Jukka Westermarck, Julia Vainonen, Päivi Koskinen
Number of pages: 65 pages + five appendices
Date: 10.11.2025

Worldwide, breast cancer is the most common cancer, and the most common cancer leading to death among women. In clinic the diagnostics and treatment of breast cancers is based on biomarkers expressed by these tumors. There are four breast cancer main types and three of them can be treated by targeting these biomarkers i.e., nuclear, or transmembrane receptors expressed in breast cancer cells of each type. The fourth breast cancer main type, triple-negative breast cancer lacks all three clinically important receptors: estrogen receptor, progesterone receptor and HER2 receptor. Triple-negative breast tumors represent a minority of breast cancer cases but unfortunately patients diagnosed with this tumor type have the highest risk of recurrence and the highest mortality rate compared to patients diagnosed with other breast cancer main types. Triple-negative breast tumors are known to be very heterogenous and, there is a crucial need for novel biomarkers to diagnose and treat this complex and aggressive breast cancer type.

The role of endogenous inhibitor proteins of protein phosphatase 2A (PP2A) as potential biomarkers in human cancer are currently under an interest since, the important tumor-suppressive activity of PP2A has evidenced to be inhibited by these inhibitors in the majority of human malignancies. When overexpressed, these inhibitor proteins are known to inhibit the dephosphorylation activity of PP2A by interacting with its dimers or trimers. The target proteins of PP2A remain phosphorylated hence, in active state, which further leads to the activation of downstream signaling pathways related to proliferation of cancer cells. This master's thesis will concentrate on three PP2A inhibitor proteins: cancerous inhibitor of PP2A (CIP2A), protein phosphatase methylesterase 1 (PME-1), and protein SET (SET). For example, the overexpression of CIP2A is linked to poor prognosis among patients with basal-like triple-negative breast cancer, even more aggressive breast tumor compared to plain triple-negative phenotype.

The first aim of this thesis was to validate antibodies targeting PP2A inhibitors CIP2A, PME-1 and SET with genetic approach in western blot. Antibodies are one of the most important tools used universally in the field of molecular biology. Unfortunately, antibodies are causing considerably problems in reproducibility and, there are no standardized methods or reporting practices to assess the validity of these tools. To validate the antibodies with genetic strategy, siRNA technique was used to produce MDA-MB-231 cells knock-down against the PP2A inhibitor of interest. Based on the validation criteria used in this thesis, all three antibodies are trustworthy to use.

The other aim was to examine the expression of CIP2A, PME-1 and SET across TNBC cell lines, both at mRNA and protein level. For this purpose, 18 triple-negative breast cancer cell lines, representing seven transcriptomic subtypes, were studied. The expression studies showed how at mRNA level, all three PP2A inhibitors overlapped since, these were overexpressed across majority of TNBC cell lines and within TNBC subtypes. But interestingly at protein level, CIP2A dominates over PME-1 and SET being only inhibitor protein overexpressed among majority of TNBC cell lines and within all TNBC subtypes. Therefore, the CIP2A protein is the most relevant PP2A inhibitor considering TNBC. In addition, CIP2A seems to be a potential novel biomarker for the invasive mesenchymal stem-like subtype, which expressed CIP2A protein at particularly high level compared to other TNBC subtypes.

Key words: Antibody, Antibody validation, Triple-negative breast cancer, PP2A, CIP2A, PME-1, SET

Table of contents

Appendix 4 Western blot

Appendix 5 RT-qPCR

1 Introduction

Breast cancer is the most common cancer globally, and among women worldwide, it is the most common cancer leading to death (International Agency for Research on Cancer, 2024). Fifteen to twenty percent of breast tumors express the triple-negative phenotype, representing a breast cancer subtype that lacks all three therapeutically important targetable receptors (The Cancer Genome Atlas Network, 2012; Livasy, 2017). Although breast tumors with this triple-negative status represent only a minority of breast cancer cases, the mortality rate is the highest when considering all breast cancer subtypes (Schneider et al., 2008). Thus, there is a crucial need for novel biomarkers providing clinically important knowledge about this aggressive and fatal breast cancer type.

Endogenous inhibitor proteins of protein phosphatase 2A (PP2A) and their role as potential biomarkers are currently under of interest. There is evidence that the tumor-suppressive activity of PP2A is inhibited by these inhibitors in the majority of human malignancies (Kauko & Westermarck, 2018), as also in triple-negative breast cancer (Laine et al., 2021).

Highly specific interaction between antibodies and their target antigens is utilized in the field of biomedicine, where antibodies are important and frequently used tools. Unfortunately, poor quality of antibodies causes significant problems in reproducibility in science, and there are no standardized validation protocols to assure their reliability (Bordeaux et al., 2010; Uhlén et al., 2016). In this master's thesis, I have validated commercial antibodies targeting endogenous inhibitor proteins of PP2A. I have also examined expression of these inhibitors across human triple-negative breast cancer cell lines.

1.1 Antibodies

In the human adaptive immune system, antibodies have an essential role in recognizing and binding antigens from pathogens or pathogen-derived toxins, with a high specificity manner (Murphy & Weaver, 2017). More closely, antibodies have two functions in vivo: to bind specifically to a pathogen or a pathogenical product that provokes an immune response, and to recruit other components of the immune system to destroy the pathogen identified and bound by the given antibody.

Antibodies of the immune system are soluble glycoprotein molecules, immunoglobulins (Schroeder & Cavacini, 2010; Trier et al. 2019). Immunoglobulins are divided into five major

isotypes (IgM, IgD, IgG, IgA, IgE) and their expression in B lymphocytes is regulated by cytokines and dependent from encountered antigens (Schroeder & Cavacini, 2010). An antigen is a molecule or a structure of the molecule that can be bound specifically to the antibody directly or through peptide fragments that are recognized by T-lymphocytes (Murphy & Weaver, 2017). Immunoglobulins are secreted into the bloodstream by plasma cells, the differentiated population of B lymphocytes. Immunoglobulins can also be bound on plasma membranes of B lymphocytes, where they form receptors for the specific antigens. With these mechanisms, immunoglobulins interact with antigens derived from pathogens and their toxic products in extracellular spaces of the body (Murphy & Weaver, 2017).

Antibody-antigen interaction occurs between the paratope site of the antibody and the epitope site of the antigen. The antigen-binding site is located in the specific domain of the paratope site, and this domain determines the antigen specificity of the antibody (Schroeder & Cavacini, 2010). This interaction requires multiple co-operative interactions to happen which gives antibodies an ability to function with high affinity and in a conformation-specific way (Trier et al., 2019). Tackling this biological nature of antibodies with progressive technologies to produce and characterize them, makes antibodies valuable and essential agents for research, diagnostics, and therapy.

For instance, in the field of molecular and cellular biology, antibodies are one of the most important research tools used universally and routinely (Bordeaux, 2010; Trier et al., 2019; Frohner et al., 2020). There are multiple immunochemical research assays, which are based on antibody-antigen interactions. For example, the western blot technique is used to separate all sample-derived proteins by their molecular weight and to transfer these to a membrane. In the membrane, the proteins of interest can be targeted and detected by using antibodies (Mahmood & Yang, 2012). Besides for research purposes, biological antibody-antigen interactions are also adapted for diagnostic use and, for prevention and therapy as antibodies are used as vaccines and therapeutic agents, respectively (Trier et al., 2019).

1.1.1 Antibody production

Both monoclonal and polyclonal antibodies are produced by applying repetitive immunization injections into an appropriate host animal (Trier et al., 2019). These injections contain the selected immunogen with an immunization-improving adjuvant agent. The goal of this immunization process is to trigger and enhance humoral immunity response, thus antibody production of the host.

While polyclonal antibodies are extracted straight from sera of different hosts, monoclonal antibodies are usually produced with a hybridoma technique where the appropriate B cells are harvested and fused with myeloma cells (Trier et al., 2019). Sera-derived polyclonal antibodies may be used in an unrefined form or after purification by different chromatography techniques, for example. Mono-specific polyclonal antibodies are obtained from the immunization process with purified antigens, and poly-specific polyclonal antibodies are produced in a process where impure mixtures of antigens are used as immunogens (Trier et al., 2012).

Needed quantities of monoclonal antibodies in turn are produced by screening hybridoma cell clones and choosing the appropriate clones for further expansion. With this technique it is potential to produce highly specific monoclonal antibodies, for which the epitope sites can be characterized (Trier et al., 2019). Also, techniques of genetic engineering, and library construction with phage display are used to produce monoclonal antibodies (Trier et al., 2012; Alfaleh et al., 2020).

1.1.2 Antibody performance

The epitope site of the immunogen determines the performance and specificity of the antibody. That is why the selected immunogen for the immunization process has a great influence on the quality of the final antibody product. Size and nature of an immunogen can be from short peptides of 10–20 amino acids to full-length proteins. When the size of the immunogen increases, the possibility for antibodies recognizing more than one epitope increases. This can be avoided by using shorter peptides or protein fragments as immunogens. (Forsström et al., 2015). The length of an epitope site is usually 5–8 amino acids, so theoretically, the risk for antibodies interacting with multiple epitopes is potential when a fragment larger than this is used as an immunogen (Trier et al., 2019).

Three-dimensional structure of an epitope site also has an influence on antibody performance. The epitope is linear when binding amino acids are located continuously, and conformational as interaction requires accurate folding of protein. This nature of the epitope can impact the application potential of antibody products as denaturation status of targeted proteins differ due to sample preparation in different assays (Forsström et al., 2015).

As the production process of polyclonal antibodies is not as refined as production of monoclonal antibodies, the risk for batch-to-batch variation and cross-reactivity increases

when using polyclonal antibodies (Trier et al., 2019). Cross-reactivity is a phenomenon where antibodies interact with different antigens with corresponding epitope sites (Schroeder & Cavacini, 2010), which can appear as off-target binding (Uhlén et al., 2016). These problems can impair reproducibility in research (Baker, 2015; Trier et al., 2019).

1.2 The importance of antibody validation

Problems in replication of results, referred to as "the replication crisis" are seen at all levels of biomedical research: basic, preclinical, and clinical (Begley & Ioannidis, 2015; Weller, 2018). It has been stated that unfortunately, most of the results presented in distinguished journals cannot be reproduced because for example, lack of proper validation (Begley & Ioannidis, 2015). Validation, by definition, is an assessment process to provide evidence that the performance of a validated concept for example, a research tool or a method, is at the required level in the context of its intended application (FDA-NIH Biomarker Working group, 2016).

It has also been stated that a majority of granted research funding is wasted for instance, due to reagents such as antibodies with poor quality (Weller, 2018). Thus, lack of proper and standardized validation protocols is wasting resources and disturbs reproducibility which further reduces reliability of science (Bordeaux et al., 2010; Frohner et al., 2020). Also, novel and potentially important information produced with validated and reproducible study protocols at basic level provide the foundation for further preclinical and clinical studies (Begley & Ioannidis, 2015).

As earlier stated, antibodies are important tools and commonly used both in basic and clinical research, and thus these reagents are expected to provide specific, selective, and reproducible results (Bordeaux et al., 2010). But unfortunately, antibodies are causing considerable problems (Weller, 2018) due to, for example, their cross-reactivity with non-target proteins, batch-to-batch variability, and unsuitable applications (Baker, 2015). While these reagents are frequently used, there are no standardized methods or reporting practices for assessing antibody validity (Bordeaux et al., 2010; Uhlén et al., 2016). This can cause misinterpretation of results or lack of reproducibility (Frohner et al., 2020) and waste of resources, both human and financial (Bordeaux et al., 2010).

1.2.1 Validation strategies for antibodies

In the context of antibodies, validation must be performed and documented properly to provide evidence that the validated antibody product is suitable for the planned purpose (Weller, 2018). The International Working Group for Antibody Validation has suggested standard guidelines for validating antibodies (Uhlén et al., 2016). They have presented five validation strategies: genetic, orthogonal, independent antibody, tagged protein expression, and immunocapture coupled with mass spectrometry, from which at least one should be used as a minimum validation criterion. Because of different sample preparation manners, conformation of proteins varies in different antibody-based assays. Thus, validation strategy should be chosen based on the study context and application (Uhlén et al., 2016).

1.2.2 Genetic validation

Genetic approach means that the gene encoding the protein of interest is knocked down or knocked out by using the small interfering RNA (siRNA) technique or the CRISPR technology, respectively (Uhlén et al., 2016). By this, the linkage between the target protein and the encoding gene can be detected. This strategy is suitable for example for western blotting where proteins are in an entirely or partly denatured form (Uhlén et al., 2016).

In this thesis, the genetic validation strategy is used to validate antibodies targeting three endogenous inhibitor proteins of protein phosphatase 2A (PP2A) by western blotting. These inhibitor proteins and their effects on PP2A activity in the context of triple-negative breast cancer are presented further. The genetic validation criteria by Uhlén et al. (2016), which are used in this thesis, are presented more closely in the methodological chapter 2.7.

1.3 Triple-negative breast cancer

According to the International Agency for Research on Cancer of World Health Organization (2024), breast cancer was the most common cancer worldwide in 2022, when considering both sexes and people of all ages. Breast cancer also killed in 2022 over 666 thousand women of all ages worldwide. Based on their molecular phenotypes, breast cancers can be classified into four main types: hormone-sensitive luminal types A and B, cancers overexpressing human epidermal growth factor receptor 2 (HER2) and, the group referred to as triple-negative (TNBC) or basal-like (BLBC) breast cancers, depending on the perspective (The Cancer Genome Atlas Network, 2012). These triple-negative/basal-like tumors form a

heterogenous group of aggressive breast cancers (Foulkes et al., 2010; Lehmann et al., 2011; The Cancer Genome Atlas Network, 2012; Denkert et al., 2017). In some contexts, TNBCs and BLBCs are referred as synonyms, although gene expression studies show evidence that this group is more complex (The Cancer Genome Atlas Network, 2012; Denkert et al., 2017). Fifteen to twenty percent of all breast tumors express this triple-negative phenotype (Denkert et al., 2017; Livasy, 2017), which lacks all three therapeutically important receptors: estrogen receptor (ER), progesterone receptor (PR) and HER2 receptor (The Cancer Genome Atlas Network, 2012).

TNBC cells have high proliferation rates (Livasy, 2017) and tumors expressing this aggressive phenotype are larger than tumors representing other subtypes (Lehmann et al., 2011). TNBCs are invasive by their nature, and thus they have poorer prognoses than hormone-sensitive subtypes (Livasy, 2017). Within five years from the first diagnosis, triple-negative breast tumors have higher risk of recurrence with metastasis when compared to other tumors types (Foulkes et al., 2010; Livasy, 2017). And as earlier mentioned, even though TNBCs represent a minority of all breast cancer cases, the mortality rate among TNBC patients is the highest when compared to patients diagnosed with other breast cancer subtypes (Schneider et al., 2008).

1.3.1 TNBC subtypes

Comprehensive gene studies by Lehmann et al. (2011) have evidenced that a diverse group of TNBCs includes six tumor phenotypes, due to their different gene expression profiles and gene ontologies (Table 1) Also few cell lines in their study cannot classified because these shared similarities with several other subtypes and, referred as unclassified. The human TNBC cell lines examined in this master's thesis are grouped by this classification and, are presented more precisely in appendix 1, Table A1.

Table 1. Triple-negative breast tumors can be classified into six subtypes based on their gene expression and the involvement of these genes (Lehmann et al., 2011). Unclassified cell lines shared similarities with several subtypes.

Transcriptomic subtype	Gene signature
Basal-like 1	Cell cycle Cell proliferation Elevated DNA damage response
Basal-like 2	Growth factor signaling Glucose metabolism
Luminal AR	Hormonally regulated pathways, including steroid synthesis and androgen receptor (AR) signaling
Unclassified	Cell lines within this subtype had similarities with several subtypes
Immunomodulatory	Immune cell signaling Antigen processing and presentation
Mesenchymal Stem-like	Cell motility, for example epithelial-mesencymal transition Cell differentiation and growth Stem cell markers
Mesenchymal-like	Cell motility, for example interaction with extracellular matrix receptors Cell differentiation and growth

Approximately 75–80 % of tumors with triple-negative status are expressing basal markers, for example, certain types of cytokeratin or epidermal growth factor receptor EGFR. These basal-like triple-negative breast cancers are even more aggressive than tumors with a bare triple-negative status (Foulkes et al., 2010; The Cancer Genome Atlas Network, 2012; Denkert et al., 2017). Basal-like cancer cells are known to have high genome instability, and large amounts of these tumors have amplification of the gene encoding the transcription factor c-MYC (The Cancer Genome Atlas Network, 2012).

1.3.2 Clinical breast cancer biomarkers

According to the National Cancer Institute, NCI (2022), a biomarker is a biological molecule, occurring in body fluids or tissues, which can implicate either normal or abnormal state of the body. Biomarkers may be for example nucleic acids, peptides, proteins, metabolites, or chemically modified biomolecules (Henry & Hayes, 2012; Goossens et al., 2015). In research areas aimed for personalized medicine, such as in the field of cancer research, whole transcriptomics, proteomics, or metabolomics can be considered as omics-based biomarkers (Rossi et al., 2022). Thus, the biomarker can be a single variable or a specific molecular signature (Ballman, 2015). Gene sequence variations which are inherited to the next

generation, can act as genetic biomarkers, and be observed from the germline genome (Henry & Hayes, 2012). On the other hand, DNA mutations detected from tumor-derived cells can serve as potential somatic biomarkers.

Biomarkers are in a central role in diagnostics and treatment of patients with breast tumors (Duffy et al., 2017. The already mentioned three targetable tissue-based markers, ER, PR and HER2, form the cornerstone for the clinical management process of breast cancer. Thus, the detection and measurement of these three receptors is the fundamental policy (Duffy et al., 2017). Breast tumors expressing these biomarkers are treatable with specific targeted therapy options (Schneider et al., 2008; Foulkes et al., 2010).

More closely, three groups of clinical cancer biomarkers are diagnostic, prognostic, and predictive (Goossens et al., 2015). Expression status of ER/PR and HER2 in breast cancer cells can be used both as a diagnostic and a predictive biomarker (Goossens et al., 2015; Duffy et al., 2017). For HER2-positive breast cancer, expression status of HER2 functions also as a prognostic biomarker (Goossens et al., 2015). Expression levels of these three receptors predict sensitivity of tumors for targeted therapy agents. Functions of the steroid receptor ER and PR can be restricted with endocrine therapy, such as selective estrogen receptor modulator tamoxifen (Duffy et al., 2017). Breast tumors with HER2 overexpression or amplification can be treated with humanized monoclonal antibody trastuzumab which inhibits protein tyrosine kinase activity of HER2 (Garnock-Jones et al., 2010; Goossens et al., 2015; Duffy et al., 2017).

Due to lack of all these three important targetable receptors, there are currently no targeted therapy options available for all patients with TNBC (Foulkes et al., 2010). Only non-targeted cytotoxic chemotherapy can be used, but unfortunately, studies have shown that not all triple-negative tumors respond to chemotherapy (Schneider et al., 2008; Foulkes et al., 2010). Programmed cell death protein (PD-1) or its ligands (for example PD-L1) can nowadays be targeted with antibody treatment, and these are currently used as a part of chemotherapy for patients with PD-L1 positive TNBC (Finnish Breast Cancer Group, 2024). Unfortunately, approximately only 20 % of triple-negative tumors express PD-L1 (Mittendorf et al. (2014).

Given the heterogeneity of the TNBC subtype, its proliferative nature and lack of targeted treatment options, there is a strong need for further information about the molecular hierarchy of this aggressive and fatal breast cancer type. Molecular analysis of this complex breast

cancer type could provide crucial knowledge to identify potential novel clinical biomarkers for diagnostic, predictive, and/or prognostic purposes.

1.4 Protein phosphatase 2A

Enzymatic activity of proteins, participating in complex intracellular signaling pathways, is regulated through diverse post-translational modifications, such as phosphorylation and methylation. Disruptions in regulation of these signaling pathways can lead to formation of a disease, such as a cancer. (Eichhorn et al., 2009.) Particularly, reversible phosphorylation of proteins, catalysed by antagonistic enzymes, is an essential contributive phenomenon in the regulation process (Westermarck & Hahn, 2008). Balance between phosphorylation and dephosphorylation activities of kinases and phosphatases, respectively, regulates the phosphorylation status, and thus also the oncogenic potential of a protein (Westermarck, 2018).

Protein phosphatase 2A (PP2A) is one of the most active serine/threonine phosphatases, expressed in all eukaryotic cells (Longin et al., 2008; Eichhorn et al., 2009; Khanna et al., 2013). By its dephosphorylation activity, it regulates phosphorylation status, hence the activity state of many proteins participating in important signaling pathways related to gene expression, replication, and apoptosis, for example (Longin et al., 2008; Khanna et al., 2013).

More closely, protein phosphatase 2A (PP2A) refers to the conserved family of serine/threonine (Ser/Thr) protein phosphatases expressed widely among eukaryotic cells (Westermarck & Hahn, 2008). It consists of a core enzyme composition with structural subunit A and catalytic subunit C. This AC dimer further assembles with regulatory subunit B, forming a heterotrimeric holoenzyme structure (Figure 1) (Westermarck & Hahn, 2008; Westermarck & Neel, 2020). Structural subunit A is one of two isoforms, Aα or Aβ encoded by *PPP2R1A* and *PPP2R1B*, respectively. It scaffolds one C subunit, either isoform Cα or Cβ encoded by *PPP2CA* and *PPP2CB*, respectively (Westermarck & Hahn, 2008). The active site of the catalytic subunit targets Ser/Thr phosphosites for dephosphorylation by hydrolysis (Eichhorn et al., 2009). B subunits regulate not only substrate specificity but also localization of PP2A holoenzyme in cell (Westermarck & Hahn, 2008).

Regulatory subunit B is one of fifteen isoforms from four B subunit families: B55, B56, PR72 and STRN, including several splice variants. Each regulatory subunit B families have different substrate profiles (Westermarck & Neel, 2020), so given the great variety of these

subunits and the variability in possible PP2A holoenzyme trimers, the substrate specificity of PP2A is diverse (Leonard et al., 2020).

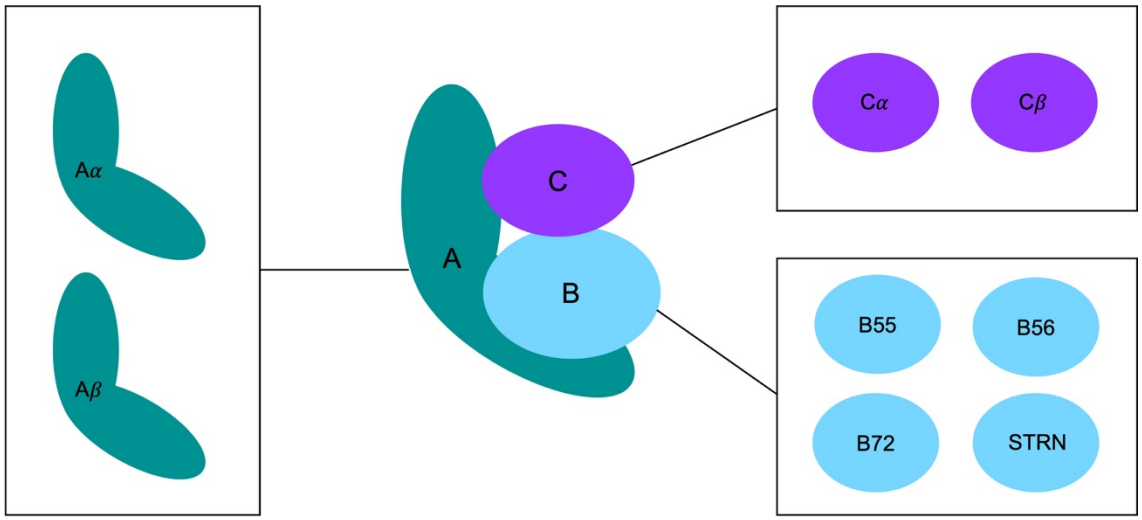

Figure 1. Protein phosphatase 2A (PP2A) is a diverse family of trimeric holoenzymes with dephosphorylation activity towards Ser/Thr residues. The trimeric structure of PP2A consists of core enzyme composition with a structural subunit A and a catalytic subunit C. The structural subunit A is either the isoform Aα or Aβ, which scaffolds either catalytic subunit Cα or Cβ. This AC dimer further assembles with a regulatory subunit B forming heterotrimeric holoenzyme structure. The regulatory subunit B is one of fifteen isoforms from four B subunit families: B55, B56, PR72 and STRN, including several splice variants within each family. As each of these regulatory subunit B families have different substrate profiles, the substrate specificity of PP2A is diverse.

The attachment of a given B subunit to the AC dimer is dependent on the post-translational methylation status of the carboxyl-terminal tail (Eichhorn et al., 2009; Kaur & Westermarck, 2016). A possibility of AC dimer binding with tumor suppressive B subunits, for example, from families of B55 or B56, is regulated enzymatically through the methylation status of Leu309 in C subunit (Figure 2). Leucine carboxyl methyltransferase 1 (LCMT1) catalyses methylation of the carboxyl group of the C-terminal Leu309 residue in subunit C, which enables formation of tumor suppressive PP2A-B55 and PP2A-B56 complexes. Demethylation of this Leu309 residue is catalysed by protein phosphatase methylesterase 1 (PME-1) which, when overexpressed, has an oncogenic role as an inhibitor of PP2A. This function of PME-1 is described in more detail in chapter 1.5.2.

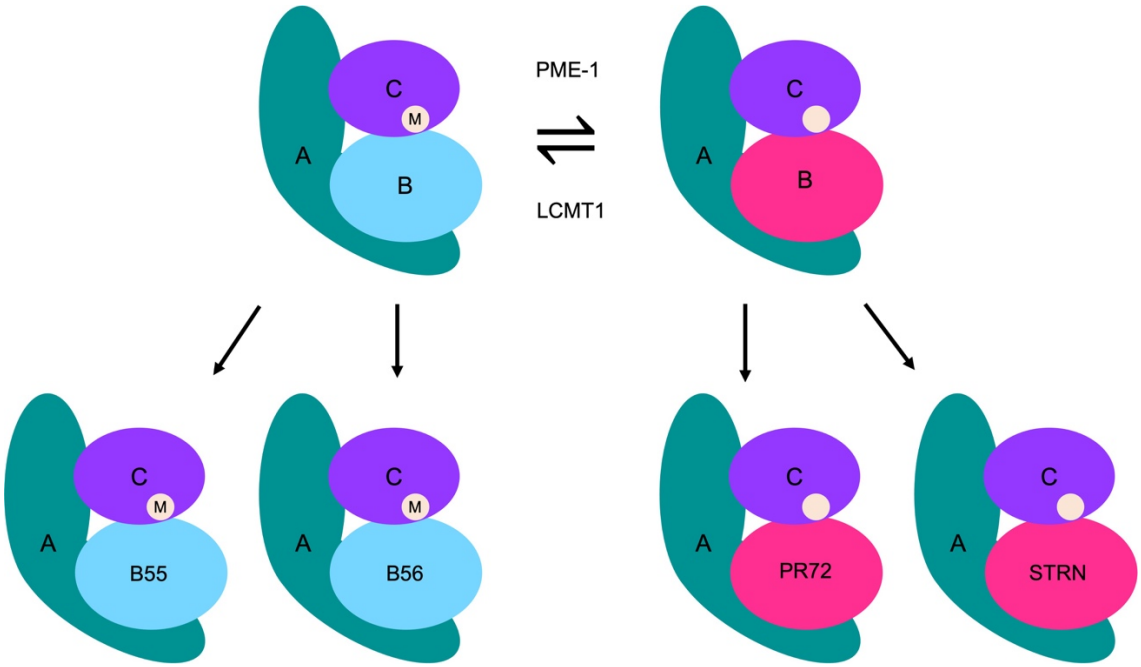

Figure 2. The attachment of the regulatory B subunit to the AC dimer is regulated post-translationally. The methylation status of the Leu309 residue, located in the carboxy-terminal of catalytic subunit C is regulated enzymatically. Leucine carboxyl methyltransferase 1 (LCMT1) catalyses the methylation (M in the C-subunit) of Leu309 residue, which enables formation of PP2A-B55 and PP2A-B56 complexes. These PP2A complexes have an important role as tumor suppressors by dephosphorylating oncoproteins. Protein phosphatase methylesterase 1 (PME-1) catalyses the demethylation (lack of M in the C-subunit) of Leu309 residue, which enables PP2A complexes PP2A-PR72 and PP2A-STRN to format. These complexes can even have oncogenic properties and therefore, when overexpressed in the cancer cells, PME-1 inhibits the crucial tumor suppressive activity of PP2A.

Therefore, PP2A has a crucial tumor suppressive role (Mäkelä et al., 2019) as it regulates activities of many oncoproteins, for example transcription factor c-MYC, which in turn induces cell proliferation (Khanna et al., 2013; Kauko & Westermarck, 2018; Leonard et al., 2020). More closely, tumor suppressive PP2A holoenzyme dephosphorylates post-transcriptionally the serine-62 residues of c-MYC (Junttila et al., 2007; Laine et al., 2013). As mentioned in chapter 1.3.1, c-MYC has an oncogenic role for example in basal-like triple-negative breast cancer cells.

1.5 Inhibitor proteins of PP2A

PP2A activity is regulated not only through the diversity in heterotrimeric structures and post-translational modifications of C-subunits, but also by endogenous proteins interacting with PP2A dimers or trimers (Niemelä et al., 2012). In cancer cells, where these inhibitor proteins are overexpressed, even when LCMT1 is normally expressed, the formation of PP2A holoenzyme complexes with tumor suppressive activity (PP2A-B55/-B56) is inhibited (Westermarck & Neel, 2020). In my master's thesis I will concentrate on three inhibitor

proteins: cancerous inhibitor of PP2A (CIP2A), protein phosphatase methylesterase 1 (PME-1), and protein SET (SET).

1.5.1 Cancerous inhibitor of PP2A

Cancerous Inhibitor of PP2A (CIP2A) is a human cytoplasmic oncoprotein encoded by the *KIAA1524* gene (Junttila et al., 2007). A majority of CIP2A is expressed as a dimer with the molecular size of ~150–200 kDa, and a minority as a monomer size of ~ 90 kDa (Wang et al., 2017).

Critical oncogenic role of CIP2A as an endogenous PP2A inhibitor was identified first by Junttila and colleagues (2007) as CIP2A was shown to have an ability to promote anchorage-independent cell growth *in vitro* and tumor formation *in vivo*. On a molecular level, CIP2A interacts directly with the transcription factor c-MYC, as CIP2A physically blocks the interaction between PP2A and c-MYC (Figure 3). The tumor-suppressive effects of PP2A are partly based on its ability to dephosphorylate c-MYC at a specific serine residue (Ser62). While this dephosphorylation leads to proteolytic degradation of c-MYC, overexpression of CIP2A prevents is and thereby increases c-MYC stability (Junttila et al., 2007).

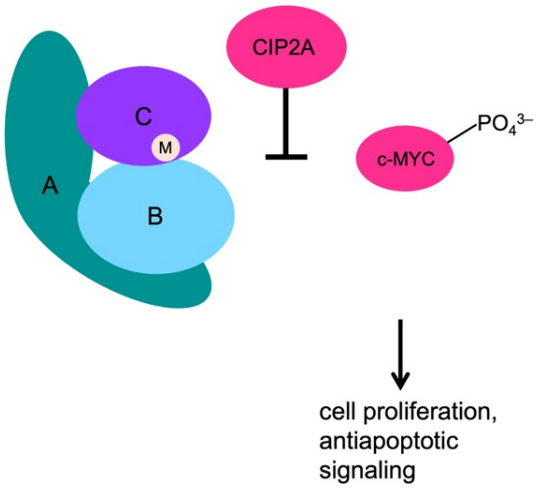

Figure 3. Cancerous inhibitor of PP2A (CIP2A) inhibits the tumor suppressive activity of PP2A by physically blocking the interaction between PP2A and oncoprotein c-MYC. CIP2A interacts directly with transcription factor c-MYC, which inhibits the dephosphorylation activity of PP2A towards c-MYC. Therefore, the target Ser62 residue of PP2A in c-MYC remains at phosphorylated state (PO_4^{3-} attached), c-MYC is stabilized and further oncogenic (e.g. cell proliferative and antiapoptotic signaling) downstream signaling pathways promoted by c-MYC are activated. Even if, the catalytic subunit C of PP2A is at methylated state (M), and AC dimer can bind tumor suppressive B-subunit, the overexpression of CIP2A inhibits the crucial tumor suppressive activity of PP2A.

This elevated activation of c-MYC in cancer through PP2A inhibition by CIP2A is the most studied (Chen et al., 2023). But at present, the role of CIP2A in cancer cell proliferation is known to be more complex. In addition to PP2A inhibition, it has been proven that CIP2A has a capability to drive growth of cancer cells by regulating phosphoproteome and inhibiting normal DNA damage response (Nagelli & Westermarck, 2024).

It has been detected that CIP2A is overexpressed in almost all types of solid tumors (Kauko & Westermarck, 2018). Also in breast cancer, the progression of disease is linked to elevated CIP2A levels. When overexpressed, CIP2A promotes chemoresistance of breast cancer cells by inhibiting normal cellular senescence mechanisms (Laine et al., 2013). Specifically, triple-negative breast cancer type, together with HER2-positive type, have the most elevated expression of CIP2A, compared to other breast cancer types (Niemelä et al, 2012). As earlier stated, these subtypes, both aggressive, also have elevated expression levels of c-MYC.

This overexpression of CIP2A both at mRNA and protein level indicates bad prognosis among patients diagnosed with basal-like triple-negative breast cancer (BL-TNBC) (Laine et al., 2021). Gene expression studies have evidenced that after five years, disease-free survival among patients having BL-TNBC with high CIP2A expression was only 40 %, while the survival percentage of BL-TNBC patients with low CIP2A expression was approximately 75 %. Also, within five years, overall survival of BL-TNBC patients with high CIP2A protein expression was only 50 %, while patients having BL-TNBC with low CIP2A expression had overall survival of approximately 85 %. Among patients diagnosed with ER-positive or non-BL-TNBC tumors, this poor prognostic effect of high CIP2A expression was not detected (Laine et al., 2021).

1.5.2 Protein phosphatase methylesterase 1

Protein phosphatase methylesterase 1 (PME-1) is an intracellular protein encoded by the conserved gene *PPME1* (Kaur & Westermarck, 2016), and is located mainly in the nucleus (Longin et al., 2008). According to the reviewed entry (Q9Y570) by the Universal Protein Knowledgebase UniProtKB (2024b), PME-1 has two isoforms sized ~ 42–44 kDa, and another two sized ~ 18–22 kDa.

As LCMT1 methylates the Leu309 residue in C-subunit (Figure 4a), PME-1 catalyses demethylation of this residue (Figure 4b). By this mechanism PME-1 not only inhibits recruitment of tumor-suppressive B subunits, but also enables assembly of AC dimer with

regulatory subunits of B subunit families of PR72 and STRN (Figure 2). Some of these PP2A-PR72 or PP2A-STRN heterotrimers can have oncogenic properties in cancer cells, where PME-1 is highly expressed or expression of LCMT1 is low. In addition, PME-1 removes manganese ions from the active site of PP2A, so catalytic activity of C-subunit is inhibited. Through all these functions, overexpressed PME-1 inhibits important tumor-suppressive activity of PP2A thus, induces proliferation of cancer cells (Kaur & Westermarck, 2016; Kauko & Westermarck, 2018; Westermarck & Neel, 2020).

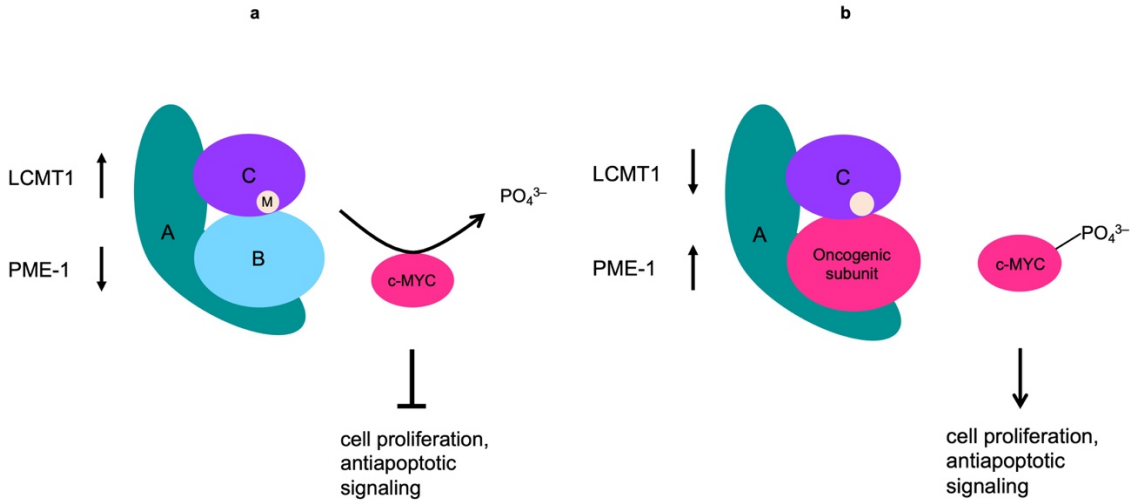

Figure 4. Overexpression of protein phosphatase methylesterase 1 (PME-1) inhibits the tumor suppressive activity of PP2A and promotes tumorigenic cell signaling. In cells (**a**) where LCMT1 is expressed at higher level compared to the expression of PME-1, the Leu309 residue of catalytic subunit C in PP2A is at methylated state (M), and tumor suppressive B-subunit (B) is recruited. PP2A catalyses the dephosphorylation (removal of PO_4^{3-} group) of Ser62 residue in c-MYC. Dephosphorylation of c-MYC enables its degradation and oncogenic signaling pathways, promoted by c-MYC, are inhibited. In cancer cells (**b**) where PME-1 is overexpressed compared to LCMT1, the Leu309 residue of catalytic subunit C in PP2A is at unmethylated state, and AC dimer assembles with B-subunits with oncogenic properties (Oncogenic subunit). Recruitment of this kind of B-subunit alters the substrate profile of PP2A so that Ser62 residue of c-MYC remains at phosphorylated state (PO_4^{3-} attached). Degradation of c-MYC is inhibited and c-MYC is stabilized hence, signaling pathways related to cell proliferation and anti-apoptosis are activated.

Function of PME-1 as an oncoprotein has been studied earlier, for example in lung cancer and gastric cancer cell lines, where the link between *PPME1* amplification and cell proliferation was proven (Li et al., 2014). But interestingly, high PME-1 expression is also linked to better prognosis among patients diagnosed with rectal cancer (Kaur et al., 2015). So, the role of PME-1 in human malignancies is not completely understood.

1.5.3 Protein SET

The protein SET (SET) is expressed widely in every cell type, mainly in the nucleus but also in other intracellular compartments (Zhao et al., 2023). According to Tozuka et al. (2021) SET has a molecular weight of 39 kDa while, according to the reviewed UniProtKB (2024c) entry (Q01105), there are four known protein isoforms sized ~ 31–33 kDa, due to by alternative splicing.

SET is associated with various cell signal pathways, including cascades regulated by PP2A. As an endogenous inhibitor of PP2A, SET interacts physically with the catalytic C subunit of PP2A (Figure 5) (Kauko & Westermarck, 2018). Therefore, when overexpressed, SET promotes tumorigenesis by increasing activation of downstream cell signaling pathways related to cell proliferation and antiapoptotic signaling (Westermarck & Hahn, 2008; Kauko & Westermarck, 2018). As CIP2A, also SET has a stabilizing effect towards c-MYC. More precisely, through a positive feedback loop between c-MYC and SET, c-MYC regulates SET expression which, in turn, stabilizes c-MYC (Kauko & Westermarck, 2018). SET is the most dominant when compared to CIP2A and PME-1, and it regulates approximately 30 % of all target phosphopeptides of PP2A (Tozuka et al., 2021).

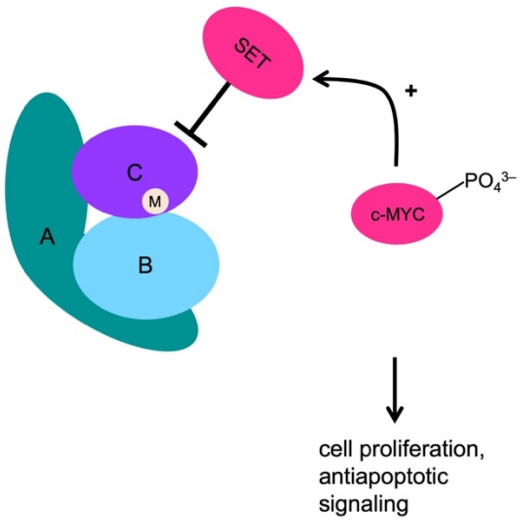

Figure 5. Protein SET (SET) stabilizes oncoprotein c-MYC through a positive feedback loop. Protein SET inhibits the dephosphorylation activity of PP2A towards its substrates by interacting physically with the catalytic subunit C. Therefore, the c-MYC is stabilized as its Ser62 residue remains at phosphorylated state (PO_4^{3-}). Further, c-MYC promotes the expression of SET which, in turn, stabilizes c-MYC. Thus, when overexpressed, SET promotes tumorigenesis by increasing activation of downstream cell signaling pathways related to cell proliferation and antiapoptotic signaling.

Elevated levels of SET have been detected in various cancer types, both solid and haematological (Tozuka et al., 2021). Also, in several cancer types, overexpression of SET is linked to drug resistance and indicates poor prognosis for a patient. Liu and colleagues (2019) have found out that SET mRNA was overexpressed in TNBC tissues and also, that SET mRNA level correlated with CIP2A levels. According to Tozuka et al. (2021) SET promotes motility and stemness of TNBC cells MDA-MB-231. This cell line represents the mesenchymal stem-like phenotype and is also examined in this thesis.

1.6 The aim of this master's thesis

The aim of this master's thesis is:

1) to validate the commercial antibodies targeting PP2A inhibitor proteins CIP2A, PME-1 and SET with genetic strategy in western blot and,

2) to examine the expression of these PP2A inhibitors across human triple-negative breast cancer cell lines at mRNA and protein level.

As stated, overexpressed CIP2A, PME-1 and SET are shown to promote cell proliferation by inhibiting the crucial tumor suppressive activity of PP2A. The role of CIP2A and SET overexpression is known to promote the progression of TNBCs but as earlier stated, the meaning of PME-1 in human cancer is not yet fully understood. This thesis could provide more information about the expression patterns of these three PP2A inhibitors across seven triple-negative subtypes, and about their further potential roles as oncoproteins in this aggressive and heterogenous form of breast cancer.

As earlier told, while antibodies are important tools used at every level of research, these reagents cause major problems in reproducibility and waste of resources. Also, no standardized methods to validate antibodies are in routine use in the field of science. In this thesis the validity of commercial antibodies targeting PP2A inhibitors CIP2A, PME-1, and SET are assessed to study the expression of these inhibitors with reliable way. And also, to evaluate if these commercial antibodies are trustworthy to use in further studies.

2 Material and methods

In this master's thesis, I validated commercial antibodies targeting three PP2A inhibitor proteins, CIP2A, PME-1 and SET, by western blotting. I used a genetic approach as a validation strategy and for this purpose, I used RNA interference to knock down the expression of the PP2A inhibitors in triple-negative breast cancer (TNBC) cells. I also examined their expression across human TNBC cell lines both at protein and mRNA level. I studied protein expression by western blotting, which is a method based on antibody-antigen interaction. The mRNA expression of the genes (*CIP2A*, *PPME1* or *SET*) encoding PP2A inhibitors I measured by quantitative reverse transcription polymerase chain reaction (RT-qPCR).

2.1 Cell lines and cell culture

For antibody validation purpose, I cultured the human-derived mesenchymal stem-like TNBC cell line MDA-MB-231 in Dulbecco's Modified Eagle's Medium (DMEM) -high glucose medium (Sigma-Aldrich or Thermo Fischer Scientific) supplemented with 10 % inactivated fetal bovine serum (FBS) and 1 % penicillin/streptomycin. I also added 1 % L-glutamine to media lacking it. When passaging the cells, I removed old medium by suction, washed the cells with Dulbecco's Phosphate Buffered Saline (Biowest) and detached them by trypsinization using Trypsin 0.25 % -EDTA in HBSS (Biowest) at 37 °C, 5 % CO2.

For both gene and protein expression studies, I used frozen pellets of 18 human derived TNBC cell lines and of the non-tumorigenic cell line MCF10A. The cell lines and cell pellets were provided by Julia Vainonen from our group. The 18 TNBC cell lines represent six transcriptomic subtypes presented by Lehmann et al. (2011). More information about TNBC cell lines and their culture conditions is provided in appendix 1, Table A1 and A2, respectively. Cell culture conditions were provided by Julia Vainonen.

2.2 Production of knock down cells by RNA interference

To validate antibodies targeting PP2A inhibitors by a genetic strategy, I produced knock down (KD) cells by RNA interference (RNAi) using small-interfering RNAs (siRNAs) specific for each gene. At seeding day (day 0), I plated MDA-MB-231 cells in DMEM to culture dishes (d = 20 cm) so that four dishes per treatment (control/siRNA) were prepared. I also produced a cell microarray tool for further protein expression and antibody validation

purposes. That is the reason why I used this scale of size to acquire the required cell amount of 30–40 x 106 cells at harvesting day. I optimized the plating dilution depending on the confluency status of original plates and the siRNA treatments that I planned to perform.

At transfection day (day 1), I removed old medium from plates with suction. After this, I pipetted 8 ml reduced serum medium Opti-MEM™ (Cat. #31985070, Gibco™) and 2 ml transfection mixture to each plate. The concentration of siRNA/control sequence in each plate was 25 nM. I incubated plates for 4 h at 37 ℃; 5 % CO2. After this I added 2X supplemented DMEM to plates. At day 2 (+ 24 h from transfection) I removed the medium with the transfection mixture and added fresh 1X supplemented DMEM to plates.

I prepared transfection mixtures with siRNA/control sequence and Oligofectamine™ 2000 transfection reagent (Cat. #12252011, Invitrogen™), and performed treatments according to an siRNA protocol used earlier by Srikar Nagelli in our group. At first, I tested this protocol for a 6-well scale and then validated it for the needed scale. The siRNA protocol is provided in appendix 2, Table A3. The sequences of control and siRNA targeting CIP2A, PME-1 and SET used for treatments were provided by our group and are presented in Table A4.

At day 3–4 (+ 48–72 h) depending on used siRNA treatment, I harvested approximately 30–40 x 106 MDA-MB-231 cells per treatment by trypsinization. For antibody validation purposes, I also pelleted 1 x 106 cells from every treatment and stored them in -80℃ until protein extraction.

2.3 Total protein and nucleic acid isolation

For expression studies, I isolated proteins, DNA, and RNA from TNBC and MCF10A pellets by using the NucleoSpin TriPrep kit (Macherey-Nagel) according to manufacturer's protocol. At lysis point, I homogenized the samples by using a syringe and an 18-gauge size needle. Because the pellets were large, I made two extractions from one pellet. Finally, I combined these two flowthroughs into one sample. so that after protocol I had samples including total protein, DNA or RNA representing each cell line.

To measure nucleic acid concentrations in these flowthroughs, I used the NanoDrop™ 2000/2000c Spectrophotometer (Thermo Scientific). I assessed the purity of nucleic acid samples based on ratio of absorbance at 260 nm and 280 nm, according to manufacturer's manual. For DNA 260/280 ratio of ~ 1.8 and for RNA ~ 2.0 was used. I continued with protein pellets and RNA elutes, and preserved DNA elutes for possible further studies.

I resuspended protein pellets with 150 μl urea/Tris buffer. After resuspension, I sonicated the protein samples for 5 minutes in ice bath with Bioruptor (Cosmobio) by using 30 seconds intervals. Then, samples were shaken for 30 minutes with 700 rpm at 37 ℃ and centrifuged with maximum speed (16.1 x 1000 rcf) at 4 ℃ for 5 minutes. I determined protein concentrations of supernatants by the Bradford assay. Unfortunately, when I used the urea/Tris buffer, the samples precipitated and were driven poorly in sodium dodecyl-sulfate polyacrylamide gel electrophoresis (SDS-PAGE), so that inconsistent bands were detected when I used antibodies against CIP2A or the loading control (β-actin).

Therefore, I lysed new frozen cell pellets from the same 18 TNBC cell lines with 150 μl RIPA buffer (appendix 3, Table A5) supplemented with phosphatase (PhosSTOP Phosphatase Inhibitor Cocktail Tablet, Roche) and protease inhibitors (cOmplete Tablet, Mini Protease Inhibitor Cocktail Tablets, Roche). These additional cell pellets were provided by Julia Vainonen.

I incubated lysates for 20 minutes on ice and vortexed them in every 5 minutes. After incubation, I sonicated lysates for 10 minutes in ice bath followed by centrifugation with the maximum speed at 4 ℃ for 30 minutes. I measured the absorbances (λ = 570 nm) of supernatants with the Pierce™ BCA Protein Assay Kit (Cat. #23227, Thermo Scientific) according to manufacturer's protocol, and by using spectrophotometer (Multiskan Ascent, Thermo Scientific). I used the standard curve method to calculate the protein amounts based on the absorbance values.

For antibody validations, I lysed cell pellets harvested from siRNA treatments with 50 μl volume of RIPA buffer supplemented with protease and phosphatase inhibitors. The protein concentration I determined by using the BCA assay and the standard curve method as described above.

2.4 Western blotting

To examine protein expression levels in KD cells and across TNBC cell lines, I prepared protein samples for western blotting. I incubated SDS-PAGE samples (30 μg aliquots of protein; 6X SDS buffer 4 μl, ddH2O to 24 μl) for 5 minutes at 90 ℃, following a quick chill at ice, and a quick spin with centrifuge. I loaded 20 μl aliquots of samples and 5 µl of a ladder (PageRuler™ Plus Prestained Protein Ladder, Cat. #26619, or PageRuler™ Prestained Protein Ladder, Cat. #26616, Thermo Scientific) to a gel (Mini-PROTEAN® TGX™ Precast Gel 4–

20 %, Cat. #456-1094, Bio-Rad Laboratories, Inc.). The proteins were driven in the Mini-PROTEAN® Tetra Cell system (Bio-Rad Laboratories, Inc.) with 150 V for approximately 45 minutes.

After this, I transferred separated polypeptides from gel to PVDF-membrane (Trans-Blot® Turbo Transfer Pack, Cat. #1704156, Bio-Rad Laboratories, Inc.) by using transfer protocol of 2.5 A; 20 V; 7 minutes in Trans-Blot® Turbo Transfer System (Bio-Rad Laboratories, Inc.). After transfer, I incubated the membranes for one hour at room temperature (RT) in a blocking solution (5 % milk, 0.1 % Tween in TBS) following primary antibody incubation overnight at 4 ℃ in a roller mixer.

For primary antibody incubation, I diluted primary antibodies 1/1000 in TBS with 1 % milk and 0.1 % Tween, except that anti-β-actin was diluted 1/2500. At next day, I washed membranes with the washing protocol of 5 x 3 minutes in TBS with 0.1 % Tween. I performed all washes in a roller mixer.

After washes I performed the secondary antibody incubation of 1 h, RT in roller mixer. I diluted secondary antibodies 1/5000 in TBS with 1 % milk and 0.1 % Tween. More specific information about primary and secondary antibodies is provided in appendix 4, Table A6 and A7, respectively.

After secondary antibody incubation, I washed membranes 4 x 3 minutes in TBS with 0.1 % Tween, and finally 3 minutes in TBS. I detected polypeptide bands with ChemiDoc™ Touch Imaging System (Bio-Rad Laboratories, Inc.) by using Pierce™ ECL Western Blotting Subtrate (Cat. #32106, Thermo Fisher Scientific), which I diluted according to manufacturer's instruction.

After detecting target bands, I performed antibody incubations to detect the loading control β-actin. When the size of the target protein was expected to be close to the size of β-actin, and when the host animal of the used primary antibody was the same as for the β-actin antibody, I incubated membranes for 15 minutes at RT in a roller mixer with Re-Blot Plus strong Solution (10X) stripping buffer (Merck Millipore) following 5 minutes washing in TBS with 0.1 % Tween and re-blocking. After stripping procedure, I performed primary and secondary antibody incubations to detect β-actin, as described earlier.

2.5 Synthesis of cDNA

For cDNA synthesis, I used 1 μg aliquots of RNA as templates. I incubated the mixture of RNA template and random hexamers in S1000 Thermal Cycler PCR system (Bio-Rad Laboratories, Inc.) for 5 minutes at 70 ℃ following 5 minutes at 4 ℃. After this I added 7.5 μl reverse transcriptase enzyme including master mix per reaction and incubated the samples for 10 minutes at RT following incubation in the PCR system 50 min at 42 ℃ and 15 min at 70 ℃. After synthesis, I chilled the samples quickly on ice, and prepared dilutions of 1/10 to new tubes and stored these at -20 ℃ until RT-qPCR. Used reaction components and their amounts are presented in appendix 5, Table A8.

2.6 Quantitative real-time polymerase chain reactions (RT-qPCR)

To examine mRNA expression across TNBC cell lines, I produced RT-qPCR reaction samples with 2 μl aliquots of cDNA templates and 18 μl of master mix. I pipetted samples as triplicates to 96-well plate. I also included blanks as triplicates with only master mix and nuclease-free water instead of template. Reagents used for reaction/one well volume are presented in Table A9. I used human gene *ACTB* encoding the β-actin protein as an endogenous control and the non-tumorigenic human breast cell line MCF10A as a calibrator.

RT-qPCR reactions were done according to the SYBR protocol previously used in our group. I present this protocol in Table A10. The reactions were run with the QuantStudio™ 12K Flex Real-Time PCR System (Thermo Fisher Scientific) instrument by the Finnish Functional Genomics Centre, Turku Bioscience.

For the planned RT-qPCR protocol, I validated the performance of the primers. I obtained the primer sequences for the *ACTB*, *CIP2A* and *PPME1* genes from our group. Primer sequences for *SET* I chose from literature (Liu et al., 2013). Primer sequences are listed in Table A11.

For all primers, I surveyed possible significant alignments with unspecific genes and species with Basic Local Alignment Search Tool (BLAST) by NCBI. I also tested the possibility for homo- or heterodimerization and hairpin structures by using OligoAnalyzer™ tool (Integrated DNA Technologies™) where I used ΔG value greater than -7 kcal/mol as a criterion. I also observed the melt curve plots from RT-qPCR output data so that no multiple Tm peaks were present and thus no dimerization had occurred.

2.7 Validation criteria for antibodies

To validate commercial antibodies targeting PP2A inhibitor proteins CIP2A, PME-1 and SET with genetic strategy in WB, I used the validation criteria proposed by the International Working Group for Antibody Validation, as described by Ùhlen et al. (2016) and The Human Protein Atlas (2022).

The validation principle in used genetic strategy is that the expression of the given target protein is significantly reduced in examined cells by RNA interference. In this master's thesis, I used small-interfering RNA (siRNA) technique described earlier in chapter 2.2. The validation criteria are that the antibody labelling is significantly reduced or eliminated in knock-down cells. I used downregulation of > 25 % as a limit of significance, when one siRNA was used.

2.8 Statistical analysis

From WB membranes, I quantified the relative amount of target proteins in every cell line with Fiji for Mac OS X and Microsoft Excel. Because the lack of protein sample from non-tumorigenic cell line MCF10A, the band area data was normalized with respect of band areas detected from the TNBC cell line CAL148. Then the band areas of target proteins were referenced to the band areas of β-actin. The protein expression of the target protein results from the ratio between the band area of a target protein and the band area of β-actin protein. I will discuss this more in the chapter 4.3.

From RT-qPCR data, I calculated relative quantification ($RQ = 2^{-\Delta\Delta Ct}$) of mRNA expression in every cell line with Microsoft Excel based on threshold cycle (Ct) values. The RQ value represents the fold chance of mRNA expression in TNBC cell line compared to the calibrator cell line (RQ value of 1) MCF10A.

I performed statistical analysis and graphic visualization with GraphPad PRISM 9. For every inhibitor protein (CIP2A, PME-1, SET), I tested correlation between protein expression and mRNA expression across TNBC cell lines. I also tested correlations between inhibitors across cell lines both at protein level and mRNA level. Before correlation testing, I tested the normality of given protein and gene expression data. Based on this, I used Pearson correlation for normal distributed data and Spearman correlation for nonparametric data. I used P value of 0.05 as a limit of significance.

3 Results

3.1 Genetic validation of antibodies targeting CIP2A, PME-1 and SET in western blot

I validated the antibodies, anti-CIP2A, anti-PME-1 and anti-SET, targeting human PP2A inhibitor protein CIP2A, PME-1 and SET, respectively, in western blot (Figure 6). Validation was made by using genetic strategy, based on small-interfering RNA (siRNA) specific for each gene. The validation criteria are presented in the methodological chapter 2.7.

The antibody targeting human CIP2A (anti-CIP2A) fulfilled the validation criterion, as the antibody labelling was reduced after CIP2A knock down (CIP2A-KD) on western blot. When in control cells the percentual band staining was 93 %, in CIP2A-KD cells it was 10 % (Figure 6a). Therefore, the labelling reduction was significant when reduction > 25 % was used as a limit of significance, according to the validation criteria by Úhlen et al. (2016) and the Human Protein Atlas (2022). The target band of expected size appeared corresponding the monomeric CIP2A. Also, additional bands of size > 180 kDa were detected on the CIP2A membrane.

Antibodies anti-PME-1 and anti-SET against human PME-1 and SET, respectively, fulfilled the validation criteria as the antibody labelling was eliminated entirely after the given mRNA knockdown on western blot membrane. When validated anti-PME-1, the percentual band staining was 81 % presenting control cells, and after PME-1-KD treatment the staining was one percent (Figure 6b). The band detected on the membrane represented the expected molecular weight of human PME-1.

In the context of validation of anti-SET, three bands of different sizes were detected from the control sample on the western blot membrane. The percentual band staining was 97 % from the upper band, 100 % from the middle band, and 62 % from the lower band (Figure 6c). After the SET-KD, the staining was three percent from the upper and the middle band, and two percent from the lower band.

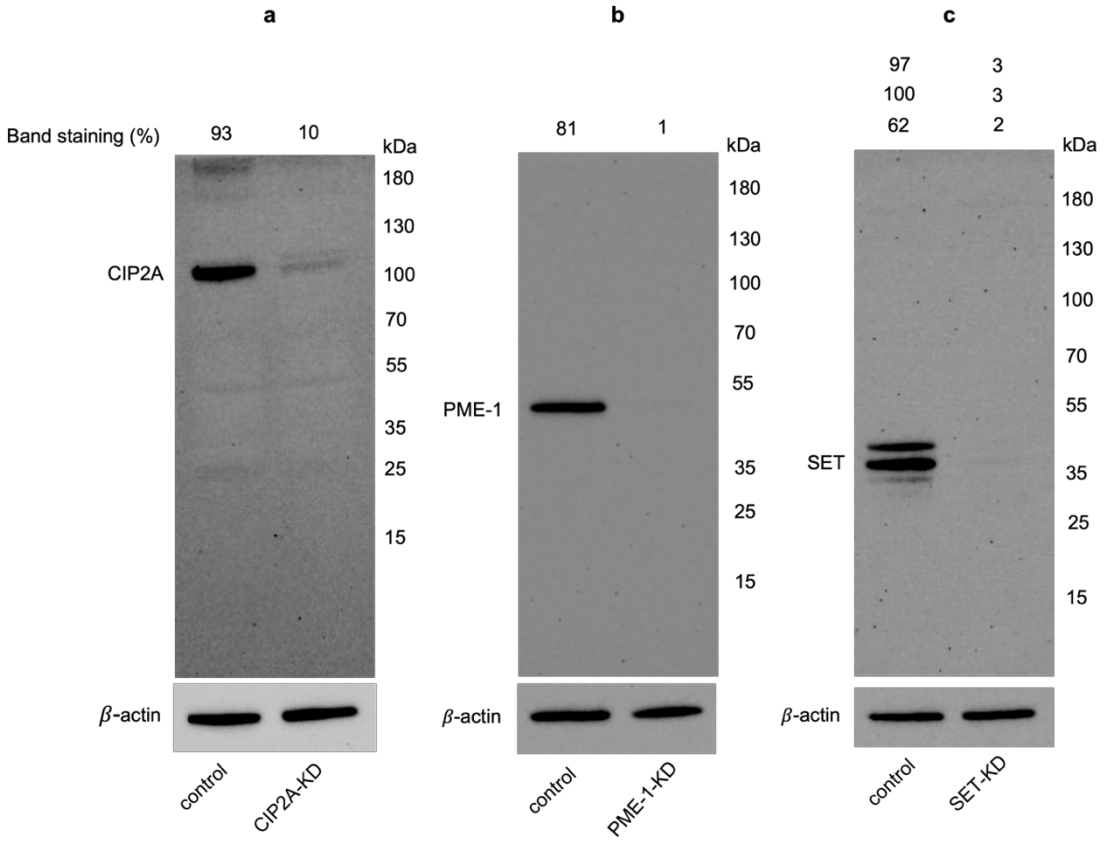

Figure 6. The antibodies targeting endogenous inhibitors of PP2A were validated in western blot by using genetic strategy. Western blot against human (**a**) CIP2A, (**b**) PME-1, and (**c**) SET compares siRNA knockdown (KD) of a given protein in human triple-negative breast cancer cell line MDA-MB-231 with control. Percentual band staining (%) is indicated. In the context of SET, the band staining is indicated so, that the top percentual value refers to the top band, the middle value to the middle band *etcetera*. Human *β*-actin is used as a loading control, and the molecular marker (kDa) is indicated on the right.

3.2 Expression of PP2A inhibitors CIP2A, PME-1 and SET across human TNBC cell lines

I also examined the expression of endogenous PP2A inhibitors CIP2A, PME-1 and SET across 18 human TNBC cell lines, both at mRNA and protein level. The cell lines are presented in appendix 1, Table A1.

3.2.1 CIP2A expression across TNBC cell lines at mRNA and protein level

The highest CIP2A mRNA expression was measured from the basal-like 2 cell line HCC1806. This cell line expressed CIP2A mRNA approximately 4.5-fold more compared to the non-tumorigenic cell line MCF10A (Figure 7a). The lowest CIP2A expression at mRNA level was detected from the mesenchymal-like cell line CAL120, which was 1.5-fold more

compared to MCF10A. Otherwise, TNBC cell lines expressed CIP2A mRNA 1.5–3.8 -fold more compared to MCF10A. All in all, every TNBC cell line expressed CIP2A mRNA more than MCF10A.

The highest, 16-fold CIP2A protein expression was quantified from the mesenchymal stem-like cell line MDA-MB-231 (Figure 7b). Also, the other mesenchymal stem-like cell lines MDA-MB-436 and the basal-like 2 cell line HCC70 expressed CIP2A protein at high level, 8.7-fold and 7.9-fold, respectively. The lowest, 0.14-fold CIP2A protein expression was quantified from the basal-like 2 cell line CAL85.

In western blot against human CIP2A protein (Figure 7c) higher signals were observed from the samples representing TNBC cell lines Hs578T, BT549, MDA-MB-436, and HCC70. This differs from the graph (Figure 7b) presenting protein expression levels, especially in the context of MDA-MB-231. I will consider this further in the discussion chapter 4.3. On the membrane pictured on the left side, lower signals were observed from the samples representing the TNBC cell lines CAL120 and CAL85. On the membrane pictured on the right side, every TNBC cell line sample, except the sample representing HCC70, were observed to give a low signal.

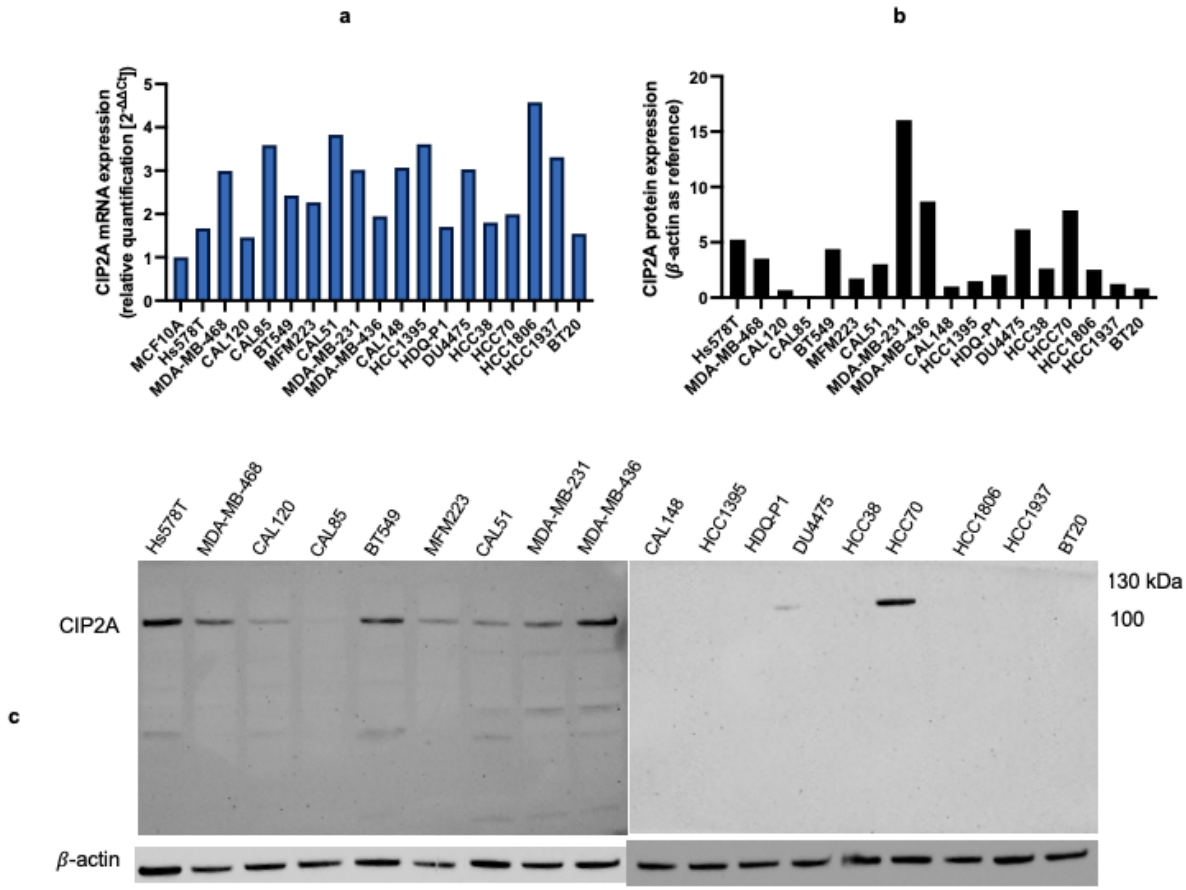

Figure 7. The expression of human CIP2A at mRNA and protein level across 18 TNBC cell lines.

(**a**) Human CIP2A mRNA expression was measured with RT-qPCR. The mRNA expression levels are presented as a relative quantification, where β-actin gene is used as an endogenous control, and the non-tumorigenic cell line MCF10A is used as a calibrator.

(**b**) Human CIP2A protein expression was quantified based on western blot. The protein expression levels are presented as a relative amount of CIP2A, where β-actin protein is used as a reference.

(**c**) The western blot against human CIP2A across 18 TNBC cell lines. β-actin is used as a loading control, and the molecular marker (kDa) is indicated.

3.2.2 PME-1 expression across TNBC cell lines at mRNA and protein level

The highest PME-1 expression at mRNA level was detected from the basal-like 1 cell line HCC38 (Figure 8a), which was approximately 2.7-fold compared to expression in the non-tumorigenic cell line MCF10A. The lowest PME-1 mRNA expression was detected from the mesenchymal-like cell line CAL51, which was approximately 0.5-fold compared to the PME-1 expression in MCF10A. Otherwise, the PME-1 mRNA expression ranged from 0.6-fold to 2.1-fold level compared to MCF10A. This means that overall, TNBC cell lines expressed PME-1 mRNA at lower levels than CIP2A mRNA and SET mRNA. Half of the TNBC cell lines expressed PME-1 mRNA more than MCF10A, and half had lower expression compared to this.

The highest expression of PME-1 protein was quantified from the mesenchymal-like cell line CAL120, which was 1.4-fold (Figure 8b). The lowest PME-1 protein expression was detected from the basal-like 1 cell line HCC1937, which was 0.09-fold. Otherwise, the expression of PME-1 protein ranged from 0.1 to 1.3.

In western blot against human PME-1 protein (Figure 8c) high signals were detected from the samples representing the TNBC cell lines MDA-MB-468, CAL120, CAL148, and DU4475. Also, the quite high signals were detected from the cell lines MFM223, HCC38, and HCC70. The lowest signals were observed from the cell lines CAL85, BT549, CAL51, HCC1395, and HCC1937.

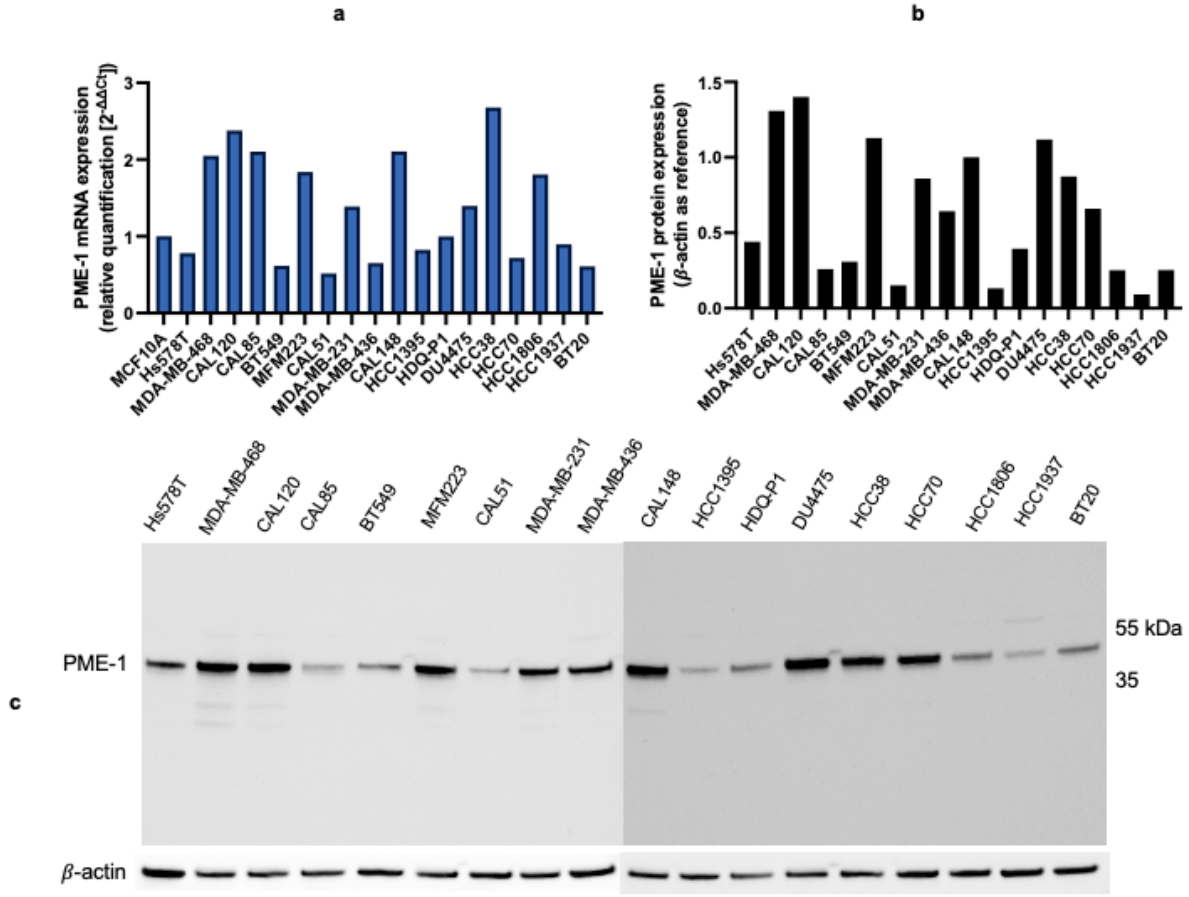

Figure 8. The expression of human PME-1 at mRNA and protein level across 18 TNBC cell lines.

(**a**) Human PME-1 mRNA expression was measured with RT-qPCR. The mRNA expression levels are presented as a relative quantification, where β-actin gene is used as an endogenous control, and the non-tumorigenic cell line MCF10A is used as a calibrator.

(**b**) Human PME-1 protein expression was quantified based on western blot. The protein expression levels are presented as a relative amount of PME-1, where β-actin protein is used as a reference.

(**c**) The western blot against human PME-1 across 18 TNBC cell lines. β-actin is used as a loading control, and the molecular marker (kDa) is indicated.

3.2.3 SET expression across TNBC cell lines at mRNA and protein level

The highest SET expression at mRNA level was detected from the luminal AR cell line CAL148 (Figure 9a). This cell line expressed SET mRNA 7.6-fold more compared to SET mRNA expression in the non-tumorigenic cell line MCF10A. The lowest SET mRNA expression was measured from the mesenchymal stem-like cell line Hs578T. The SET mRNA expression was 1.1-fold compared to the SET mRNA expression in MCF10A. Otherwise, the SET mRNA expression ranged from 1.9-fold to 4.6-fold level compared to SET mRNA expression in MCF10A.

The highest expression of SET protein quantified from the luminal AR cell line MFM223 (Figure 9b), which was 1.6-fold. The lowest expression of SET protein calculated from the unclassified TNBC cell line HCC1395, which was 0.09-fold. Otherwise, the SET protein expression detected to range from 0.1-fold to 1.0 -fold.

In western blot against human protein SET (Figure 9c) high signals were observed especially from the samples representing the TNBC cell lines MFM223, HCC70, HCC1806, and HCC1937. Lower signals were detected from the cell lines CAL51, HCC1395, and HCC38.

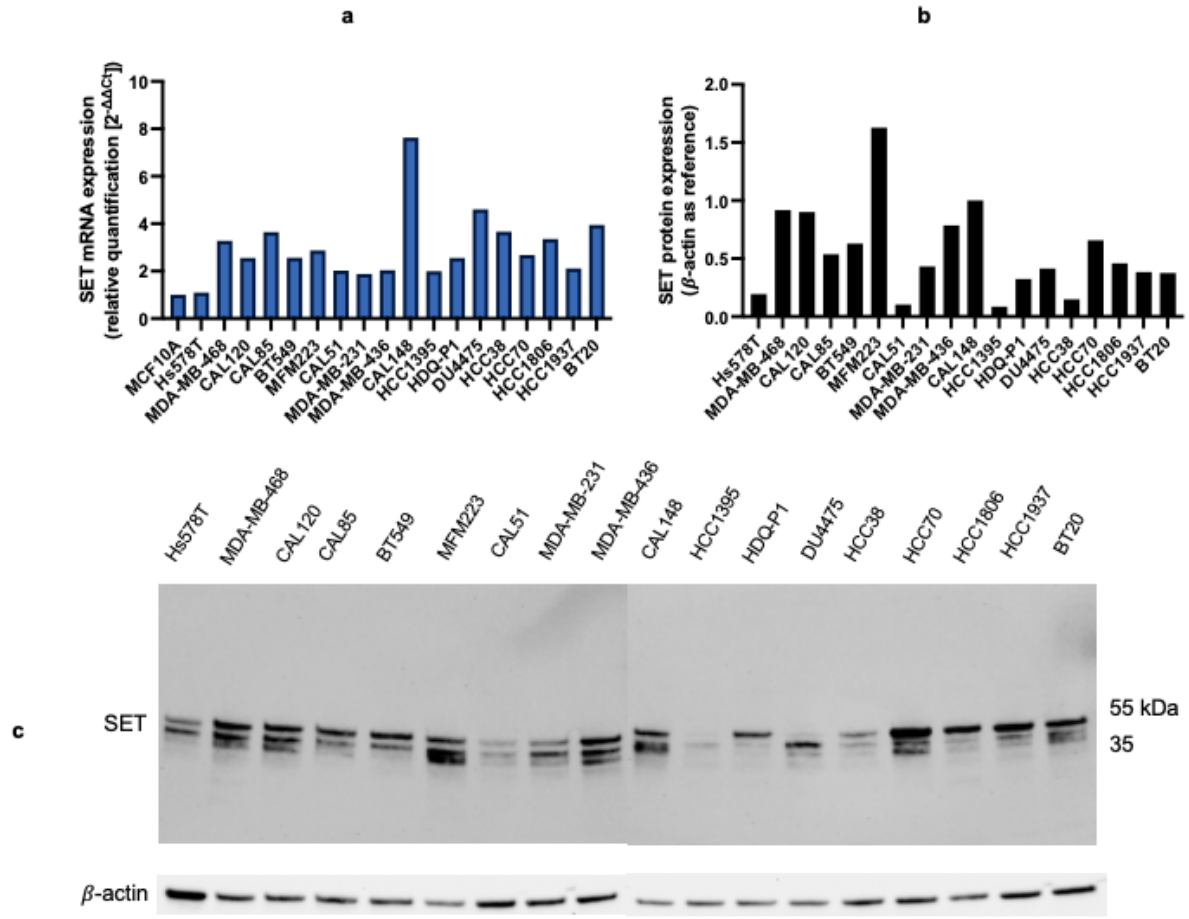

Figure 9. The expression of human SET at mRNA and protein level across 18 TNBC cell lines.

(**a**) Human SET mRNA expression was measured with RT-qPCR. The mRNA expression levels are presented as a relative quantification, where β-actin gene is used as an endogenous control, and the non-tumorigenic cell line MCF10A is used as a calibrator.

(**b**) Human SET protein expression was quantified based on western blot. The protein expression levels are presented as a relative amount of SET, where β-actin protein is used as a reference.

(**c**) The western blot against human SET across 18 TNBC cell lines. β-actin is used as a loading control, and the molecular marker (kDa) is indicated.

3.3 Mean expression of PP2A inhibitors CIP2A, PME-1 and SET between TNBC subtypes

I examined the mean expression of CIP2A, PME-1 and SET, both at mRNA and protein level, between seven TNBC subtypes: basal-like 1, basal-like 2, luminal AR, unclassified, immunomodulatory, mesenchymal stem-like, and mesenchymal-like. I grouped TNBC cell lines into these subtypes based on their transcription phenotypes determined earlier by Lehmann and colleagues (2011). These subtypes are presented in the introduction (Table 1), and the cell lines in appendix 1, Table A1.

3.3.1 Mean CIP2A expression between TNBC subtypes at mRNA and protein level

Among TNBC subtypes with two or more cell lines, the highest mean CIP2A mRNA expression was detected from the basal-like 2 subtype (Figure 10a, Table 2). The single immunomodulatory cell line DU4475 expressed CIP2A mRNA with a slightly higher level than this. The lowest mean CIP2A mRNA expression was measured from the mesenchymal stem-like subtype. Overall, the mean expression of CIP2A mRNA was detected to be quite similar between TNBC subtypes. The basal-like 1 and the luminal AR subtypes had alike mean CIP2A mRNA expressions, and so had the unclassified and the mesenchymal-like subtype. The highest deviation (SD) within CIP2A mRNA expression levels calculated between cell lines representing the unclassified subtype (Table 2). The lowest deviation within CIP2A mRNA was detected from the luminal AR subtype.

Among TNBC subtypes with two or more cell lines, the highest mean CIP2A protein expression was detected from the mesenchymal stem-like subtype (Figure 10b, Table 2). Within this subtype also, the deviation was the highest. As stated in chapter 3.2.1, the mesenchymal stem-like cell line MDA-MB-231 expressed CIP2A protein the most out of all 18 TNBC cell lines. Also, the other two cell lines representing this subtype, MDA-MB-436 and Hs578T, expressed CIP2A protein with the distinctly higher levels compared to other 18 TNBC cell lines. Among TNBC subtypes with two or more cell lines, the lowest mean CIP2A protein expression was detected from the unclassified TNBC subtype. The deviation within this subtype, considering CIP2A protein, was also the lowest.

When comparing basal-like subtypes, the basal-like 2 subtype had higher mean CIP2A protein expression than the basal-like 1 subtype, as was also detected in the context of mean CIP2A mRNA expression. However, a quite high deviation of CIP2A protein expression levels was observed between cell lines representing the basal-like 2 subtype. When compared to all 18 TNBC cell lines, CAL85 expressed CIP2A protein at the lowest, and HCC70 at the second highest level, both representing this basal-like 2 subtype.

When examined the mesenchymal origin subtypes, the mesenchymal stem-like subtype had the highest mean CIP2A protein expression among TNBC subtypes, while the mesenchymal-like subtype expressed CIP2A protein with a quite similar mean expression level compared to basal-like subtypes.

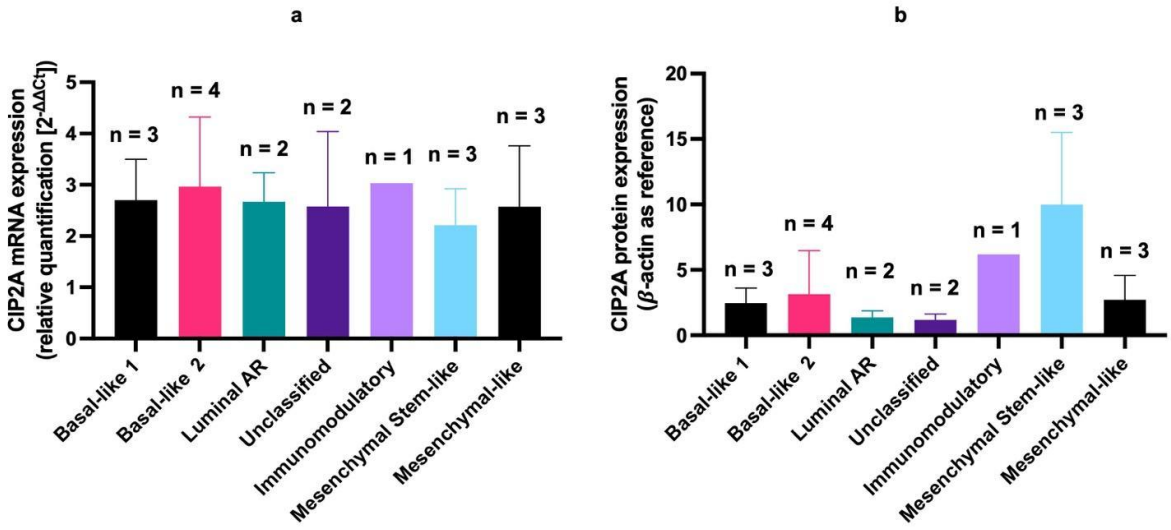

Figure 10. Mean expression of human CIP2A at mRNA and protein level within TNBC subtypes.

(**a**) Mean mRNA expression of human CIP2A within seven different TNBC subtypes. The mean values were determined based on relative quantification values derived from RT-qPCR results.

(**b**) Mean protein expression of human CIP2A within seven different TNBC subtypes. The mean values were determined based on relative target protein amounts derived from western blot results.

The bar size indicates the mean value of the expression, and the deviation is presented as error bars. The amount of cell lines within each subtype (n) is presented above the error bar.

Table 2. Mean (M) and standard deviation (SD) values representing CIP2A mRNA and protein within each TNBC subtype. The amount of cell lines within each subtype (n) is included. In this thesis only one cell line representing the immunomodulatory subtype was used, so the standard deviation was not determined (ND).

TNBC subtype	**CIP2A mRNA**		**CIP2A protein**		
	M	SD	M	SD	n
Basal-like 1	2.7	0.79	2.5	1.1	3
Basal-like 2	2.9	1.4	3.1	3.3	4
Luminal AR	2.7	0.57	1.4	0.52	2
Unclassified	2.6	1.5	1.2	0.46	2
Immunomodulatory	3.0	ND	6.2	ND	1
Mesenchymal Stem-like	2.2	0.71	9.9	5.5	3
Mesenchymal-like	2.6	1.2	2.7	1.9	3

3.3.2 Mean PME-1 expression between TNBC subtypes at mRNA and protein level

Among TNBC subtypes with two or more cell lines, the highest mean expression of PME-1 was detected from the luminal AR subtype, both at mRNA (Figure 11a, Table 3) and protein level (Figure 11b, Table 3). The lowest mean PME-1 expression was observed from the unclassified subtype, also both at mRNA and protein level.

When comparing the basal-like subtypes, both at the mRNA and protein level, the basal-like 1 had higher mean PME-1 expression than the basal-like 2, at both expression levels. Between the mesenchymal origin subtypes, a quite similar mean PME-1 expression was detected at protein level. At mRNA level, the mean PME-1 expression observed from the mesenchymal-like subtype was a slightly higher than from the mesenchymal stem-like subtype.

The highest deviation within PME-1 expression levels was detected from the mesenchymal-like subtype, both at mRNA and protein level. Within this subtype, again both at mRNA and protein level, the highest PME-1 expression was calculated from CAL120, and the lowest from CAL51. As earlier stated in the chapter 3.2.2, CAL120 expressed PME-1 protein the most out of all 18 TNBC cell lines. At mRNA level the expression from this cell line was the second highest of all cell lines. The lowest deviation within PME-1 expression levels was detected from the unclassified subtype, both at mRNA and protein level. Within this subtype, HCC1395 expressed PME-1 mRNA more than BT20, but at protein level BT20 expressed PME-1 more.

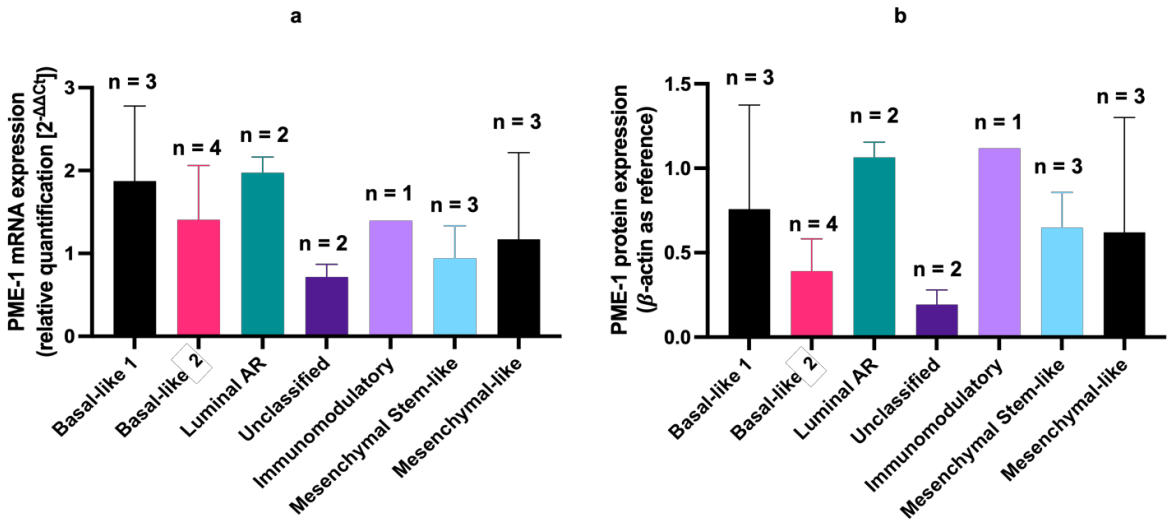

Figure 11. Mean expression of human PME-1 at mRNA and protein level within TNBC subtypes.

(**a**) Mean mRNA expression of human PME-1 within seven different TNBC subtypes. The mean values were determined based on relative quantification values derived from RT-qPCR results.

(**b**) Mean protein expression of human PME-1 within seven different TNBC subtypes. The mean values were determined based on relative target protein amounts derived from western blot results.

The bar size indicates the mean value of the expression, and the deviation is presented as error bars. The amount of cell lines within each subtype (n) is presented above the error bar.

Table 3. Mean (M) and standard deviation (SD) values representing PME-1 mRNA and protein within each TNBC subtype. The amount of cell lines within each subtype (n) is included. In this thesis only one cell line representing the immunomodulatory subtype was used, so the standard deviation was not determined (ND).

TNBC subtype	PME-1 mRNA		PME-1 protein		
	M	SD	M	SD	n
Basal-like 1	1.9	0.90	0.76	0.62	3
Basal-like 2	1.4	0.65	0.39	0.19	4
Luminal AR	2.0	0.19	1.0	0.09	2
Unclassified	0.70	0.15	0.19	0.08	2
Immunomodulatory	1.4	ND	1.1	ND	1
Mesenchymal Stem-like	0.94	0.39	0.65	0.20	3
Mesenchymal-like	1.2	1.0	0.62	0.68	3

3.3.3 Mean SET expression between TNBC subtypes at mRNA and protein level

Among seven TNBC subtypes, the highest mean expression of SET was detected from the luminal AR subtype, both at mRNA (Figure 12a, Table 4) and protein level (Figure 12b, Table 4). The lowest mean SET mRNA expression was observed from the mesenchymal stem-like subtype, and at protein level the lowest mean SET expression was detected from the unclassified subtype. The single immunomodulatory cell line DU4475 expressed SET mRNA at the second highest level, while at protein level SET expression was quite similar as mean within most of the subtypes.

Also, the highest deviation was calculated within the luminal AR subtype, again both at mRNA and protein level (Table 4). As earlier stated in chapter 3.2.3, both cell lines within this transcriptomic subtype expressed SET at the highest level of all 18 TNBC cell lines, CAL148 at mRNA level and MFM223 at protein level.

The lowest deviation in SET mRNA was detected within the mesenchymal-like subtype (Table 4), as cell lines CAL120 and BT549 expressed SET mRNA at similar level. The SET mRNA measured from the third cell line within this subtype, CAL51, differed only slightly from these two other cell lines. At protein level, the lowest deviation was calculated within the basal-like 2 subtype, where all four cell lines had a very similar SET protein level.

When comparing mean SET expression levels between basal-like subtypes, expression was similar both at mRNA and protein level. In the context of SET mRNA expression, also the deviation within both basal-like subtypes was similar. But at the protein level, the basal-like 1

subtype had higher deviation compared to the basal-like 2 subtype because as earlier stated, within this subtype the deviation was the lowest. The unclassified subtype had quite similar mean SET mRNA expression than both basal-like subtypes.

As stated, the lowest mean SET mRNA expression was observed from the mesenchymal stem-like subtype, while the mesenchymal-like subtype expressed SET at more similar level with the majority of subtypes. At protein level, both mesenchymal origin subtypes had a quite similar mean SET expression.

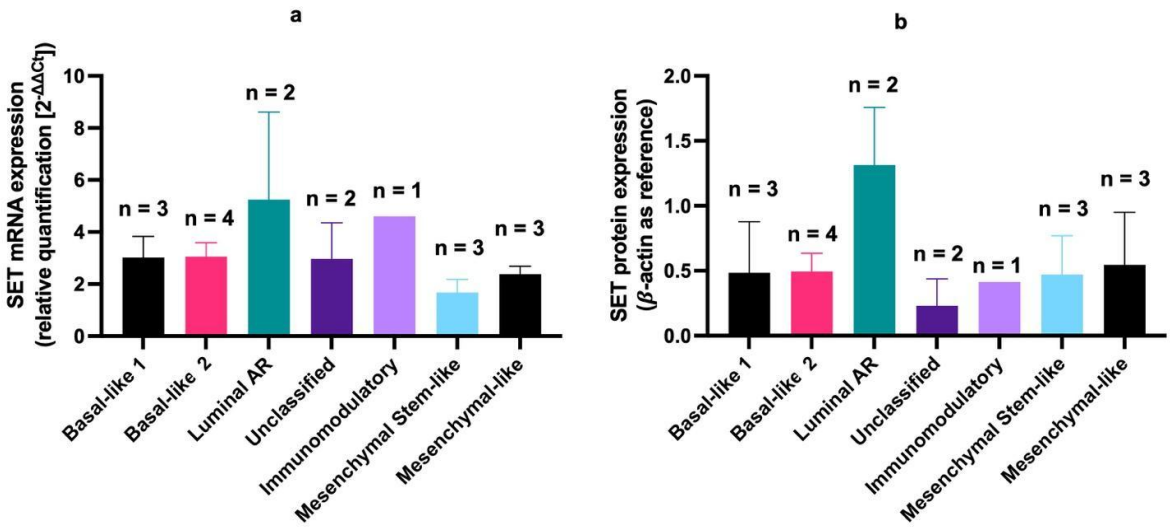

Figure 12. Mean expression of human SET at mRNA and protein level between TNBC subtypes.

(**a**) Mean mRNA expression of human SET between seven different TNBC subtypes. The mean values were determined based on relative quantification values derived from RT-qPCR results.

(**b**) Mean protein expression of human SET between seven different TNBC subtypes. The mean values were determined based on relative target protein amounts derived from western blot results.

The bar size indicates the mean value of the expression, and the deviation is presented as error bars. The amount of cell lines within each subtype (n) is presented above the error bar.

Table 4. Mean (M) and standard deviation (SD) values representing SET mRNA and protein within each TNBC subtype. The amount of cell lines within each subtype (n) is included. In this thesis only one cell line representing the immunomodulatory subtype was used, so the standard deviation was not determined (ND).

TNBC subtype	**SET mRNA**		**SET protein**		
	M	SD	M	SD	n
Basal-like 1	3.0	0.81	0.48	0.39	3
Basal-like 2	3.1	0.53	0.49	0.14	4
Luminal AR	5.2	3.4	1.3	0.44	2
Unclassified	2.9	1.4	0.23	0.21	2
Immunomodulatory	4.6	ND	0.41	ND	1
Mesenchymal Stem-like	1.7	0.50	0.47	0.29	3
Mesenchymal-like	2.4	0.31	0.54	0.40	3

3.4 Correlation between protein and mRNA expression of PP2A inhibitors CIP2A, PME-1 and SET across human TNBC cell lines

I tested correlations between protein and mRNA expression of PP2A inhibitors CIP2A, PME-1 and SET across 18 TNBC cell lines. I detected no correlation (r = -0.05; P = 0.84, where P = 0.05 was a limit of significance) between CIP2A protein and CIP2A mRNA expression across 18 TNBC cell lines (Figure 13a). In the context of PME-1, I detected a weak correlation (r = 0.37; P = 0.14, where P = 0.05 was a limit of significance) between protein expression and mRNA expression (Figure 13b). Also, between SET protein and SET mRNA expression, I detected a weak correlation (r = 0.33; P = 0.18, where P = 0.05 was a limit of significance) (Figure 13c).

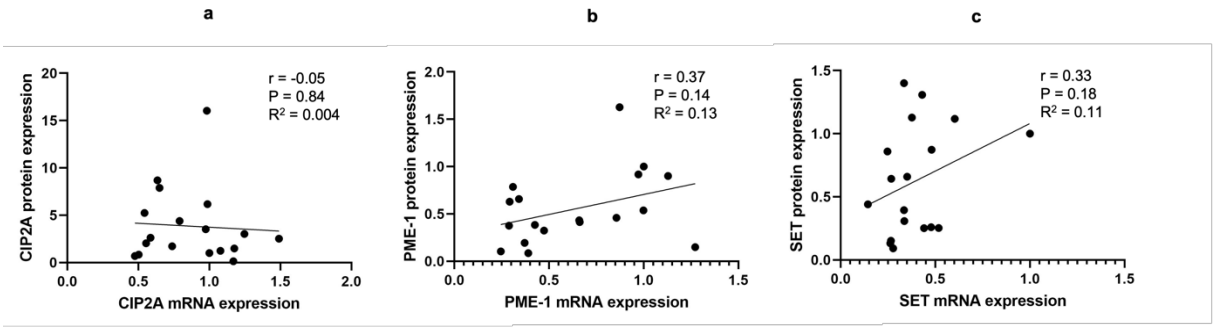

Figure 13. The correlation between protein expression and mRNA expression of PP2A inhibitors CIP2A, PME-1 and SET was tested across 18 human TNBC cell lines.

(**a**) No correlation was detected between values representing CIP2A protein expression and CIP2A mRNA expression across 18 TNBC cell lines.

(**b**) A weak correlation was detected between PME-1 protein expression and PME-1 mRNA expression across 18 TNBC cell lines.

(**c**) A weak correlation was detected between SET protein expression and SET mRNA expression across 18 TNBC cell lines.

Values representing coefficient of correlation (r), P-values (P) and coefficient of determination (R^2) for each correlation test are presented next to the given graph. For P-value 0.05 was used as a limit of significance.

3.5 Correlation between PP2A inhibitor expressions across human TNBC cell lines at mRNA and protein level

I tested correlations between expression levels of three human PP2A inhibitors across 18 TNBC cell lines. The correlations were tested between inhibitor pairs, both at mRNA and protein level. In the context of mRNA expression levels representing the genes encoding

human CIP2A, PME-1 and SET (Figure 14), no correlations were detected between inhibitor pairs. Values representing coefficient of correlation (r) and P-values (P) are presented in Table 5. P-value of 0.05 was used as a limit of significance.

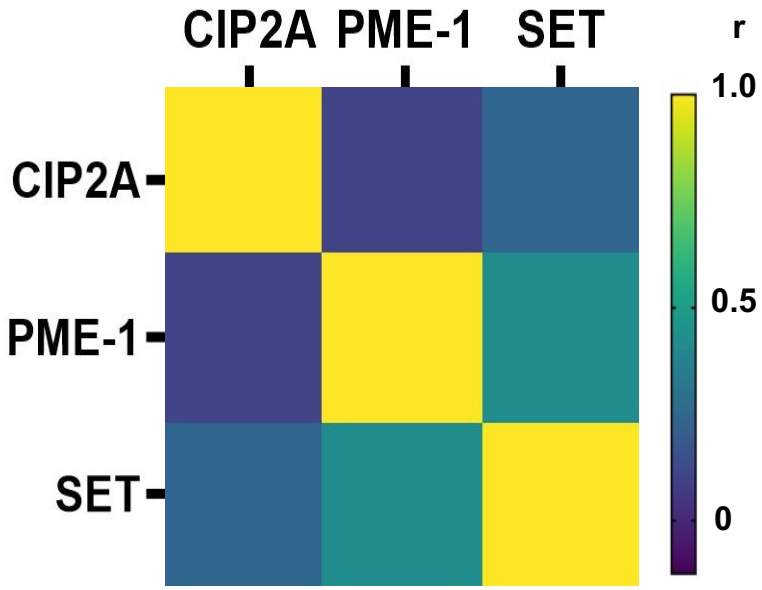

Figure 14. The correlation between mRNA expression levels of human PP2A inhibitors CIP2A, PME-1 and SET was tested across 18 TNBC cell lines. The expression levels of mRNA representing the genes encoding human CIP2A, PME-1 and SET within 18 TNBC cell lines were quantified in RT-qPCR, and the correlations between mRNA expressions of these three different inhibitors were tested. The PP2A inhibitor pairs are presented in the heat map, so that every column of the map represents one inhibitor, and every row of the map represents the other. The first column and the first row represent the CIP2A, the second arrangements represent the PME-1, and the third arrangements represent the SET. The result of each correlation test between a given inhibitor pair is presented as a certain colour, and the colour range representing the range of coefficient of correlation $0 < r < 1.0$ is presented on the right.

Table 5. The correlations between mRNA expressions corresponding to the genes encoding human PP2A inhibitors CIP2A, PME-1 and SET across 18 TNBC cell lines. Values representing coefficient of correlation (r) and P-values (P) for each correlation test are presented in the table. P-value (P) of 0.05 was used as a limit of significance. The significancy of each correlation is presented in the cell representing the P-value; not significant (ns); $P \leq 0.05$ (*); $P \leq 0.01$ (**); $P \leq 0.001$ (***).

	CIP2A		**PME-1**		**SET**	
	r	P	r	P	r	P
CIP2A			0.09	0.69; ns	0.24	0.31; ns
PME-1	0.09	0.69; ns			0.42	0.07; ns
SET	0.24	0.31; ns	0.42	0.07; ns		

When examined correlations between protein expressions of different PP2A inhibitor pairs across 18 TNBC cell lines (Figure 15) a significant correlation ($r = 0.62$; $P = 0.0057$, where $P = 0.05$ was a limit of significance) between PME-1 and SET expression (Figure 16) was detected. Between protein expressions of CIP2A and PME-1, or CIP2A and SET, no

correlation was detected. Values representing coefficient of correlation (r) and P-values (P) are presented in Table 6. P-value of 0.05 was used as a limit of significance.

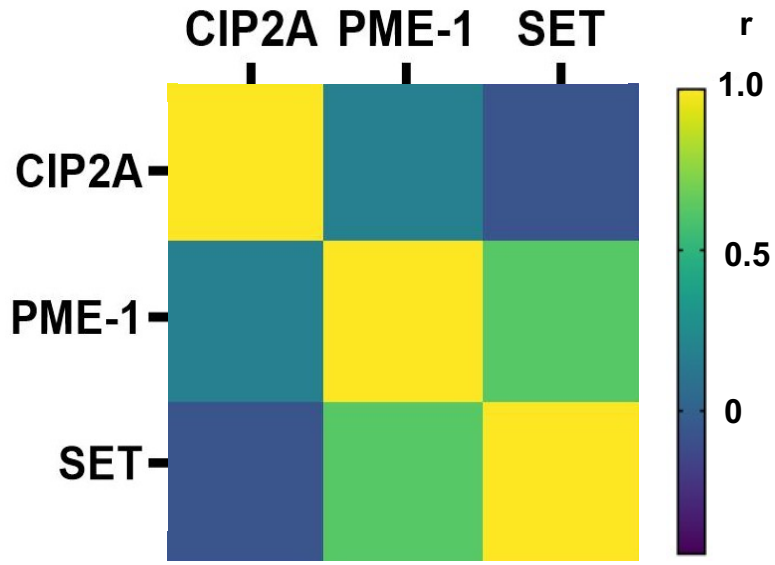

Figure 15. The correlation between protein expression levels of human PP2A inhibitors CIP2A, PME-1 and SET was tested across 18 TNBC cell lines. The expression levels of human CIP2A, PME-1 and SET protein within 18 TNBC cell lines were quantified based on band staining in western blot, and the correlation between three different inhibitors were tested. The PP2A inhibitor pairs are presented in the heat map, so that every column of the map represents one inhibitor, and every row of the map represents the other. The first column and the first row represent the CIP2A, the second arrangements represent the PME-1, and the third arrangements represent the SET. The result of each correlation test between a given inhibitor pair is presented as a certain colour, and the colour range representing the range of coefficient of correlation $0 < r < 1.0$ is presented on the right.

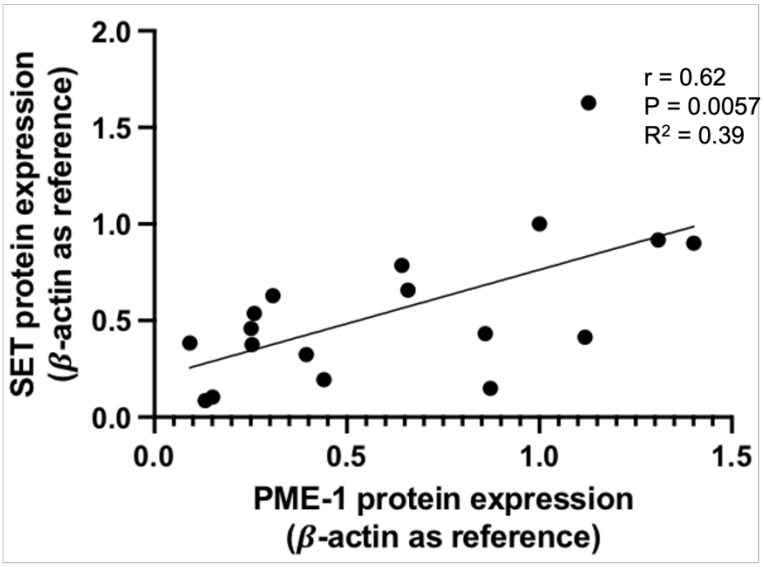

Figure 16. A significant correlation between human PME-1 and SET protein expressions was detected across 18 TNBC cell lines. Values representing coefficient of correlation (r), P-value (P) and coefficient of determination (R^2) are presented next to the graph. P-value (P) of 0.05 was used as a limit of significance.

Table 6. The correlation between protein expressions of human PP2A inhibitors CIP2A, PME-1 and SET across 18 TNBC cell lines. Values representing coefficient of correlation (r) and P-values (P) for each correlation test are presented in the table. P-value (P) of 0.05 was used as a limit of significance. The significancy of each correlation is presented in the cell representing the P-value; not significant (ns); P ≤ 0.05 (*); P ≤ 0.01 (**); P ≤ 0.001 (***).

	CIP2A		**PME-1**		**SET**	
	r	P	r	P	r	P
CIP2A			0.17	0.49	-0.08	0.77; ns
PME-1	0.17	0.49; ns			0.62	0.0057; **
SET	-0.08	0.77; ns	0.62	0.0057; **		

4 Discussion

4.1 Antibody performance

The first aim of my thesis was to validate commercial antibodies, anti-CIP2A, anti-PME-1 and anti-SET targeting PP2A inhibitor proteins CIP2A, PME-1 and SET, respectively, with genetic strategy in western blot. In the result section I showed that all three antibodies, anti-CIP2A, anti-PME-1 and anti-SET fulfilled the validation criteria. In this section I will discuss the performance and trustworthiness of each antibody based on genetic validation and in TNBC blots against of a given inhibitor.

4.1.1 Performance of anti-CIP2A

When I validated anti-CIP2A with genetic strategy (Figure 6a) I detected a band of expected size corresponding to molecular weight of monomeric human CIP2A isoform-1 sized ~ 102 kDa (UniProtKB, 2024a). This result is also similar to the product data provided by the manufacturer (Santa Cruz Biotechnology Inc., 2025a). I also observed an additional band of size > 180 kDa. When comparing the band staining between control and CIP2A-KD, the reduced labelling and therefore, reduced CIP2A expression was observed after CIP2A-KD treatment, also in the context of this given additional band. According to Wang et al. (2017) the majority of cellular CIP2A occurs both as a dimer, size of ~150–200 kDa, and as a protein complex with higher molecular weight (> 440 kDa). Therefore, these additional bands could possibly represent CIP2A dimer. As stated in the introduction, successful denaturation of proteins into polypeptides during the western blot sample preparation has an effect on three-dimensional structure of epitopes. This further affects the interaction between an antibody and an epitope site of the target protein. Considering this fact, it can be discussed if the protein samples are only partly denatured in this given assay. In the datasheet provided by the manufacturer (Santa Cruz Biotechnology Inc., 2025a), the highest molecular weight in their molecular marker is 110 kDa. Therefore, the appearance of possible CIP2A dimer cannot be detected from manufacturers data. The expression of human β-actin protein, and thus the antibody labelling was not reduced after KD, as expected.

Although, the antibody labelling representing CIP2A-KD cells is reduced significantly compared to the control cells, the difference between the percentual band staining values of CIP2A-KD and control samples is lower than the corresponding values representing the

validation result of anti-PME-1 and anti-SET. Therefore, it is possible that the transfection effect of CIP2A-KD has not been as efficient as with PME-1-KD and SET-KD.

When producing the KD-cells, I used the low-serum medium for plates when performing the transfection. If removing the old DMEM and cell washing with PBS was not done properly before the transfection, it is possible that part of the transfection complexes was inhibited by serum. This could have affected to the transfection activity. However, I used the same siRNA protocol for PME-1-KD and SET-KD treatments and, as the antibody labelling was lower in KD-cells compared to control in these validation assays, this transfection complex inhibition by high-serum environment seems unlikely. The mesenchymal stem-like cell line MDA-MB-231, which was used for validation purposes, expressed CIP2A protein at the highest level of all 18 TNBC cell lines. Also, the CIP2A mRNA expression was quite high from this cell line. So, it is more likely that CIP2A-KD treatment was not efficient enough for these cells. On the other hand, a higher amount of CIP2A-siRNA would have affected to the survival of the cells. As mentioned in methodological chapter 2.2., I performed the transfections in big scale to gather the cell pellets for cell microarray tool production. The high cell death rate would have complicated the acquiring the needed cell amount. So, as the labelling reduction was significant, the CIP2A-KD efficiency for this thesis's purpose to validate antibodies was enough.

When I examined the performance of anti-CIP2A on western blot membranes with 18 TNBC samples (Figure 7c), the target bands appeared corresponding to the expected human CIP2A molecular weight of ~ 102 kDa. This finding is similar to the genetic validation result of anti-CIP2A. I also detected light additional bands with lower molecular weight in almost all sample lanes on the TNBC membrane pictured on the left side (Figure 7c). I also observed these similar additional bands in genetic validation assay (Figure 6a) and detected no reduction in antibody labelling in these bands, when compared CIP2A-KD cells to control cells.

I found no specific validation protocols considering three primary antibodies targeting PP2A inhibitors tested and used in this thesis. Given the recognized lack of standardized methods and reporting practices for assessing antibody validity, this is not a surprise. According to manufacturer, their antibodies are optimized by using their recommended protocol (Santa Cruz Biotechnology Inc., 2025b) for western blotting. Similar to their protocol, I also used RIPA buffer to lyse proteins from TNBC cell lines. But compared to them, I used a lower

amount of whole cell lysate, sample buffer with a higher SDS concentration and longer incubation time at 90 ℃ for denaturation for sample preparation. According to manufacturer their electrophoresis was made “according to standard protocols”. Therefore, I cannot compare the SDS-PAGE conditions between the manufacturer and my thesis. For blotting, I used primary antibody dilution within the range recommended by the manufacturer.

According to Mahmood & Yang (2012) the additional bands can be cause of the protein degradation. To prevent this degradation, I supplemented RIPA buffer with protease inhibitor cocktail, but if the buffer solution was not fresh enough, it is possible that the additional bands with lighter molecular weights are CIP2A derivatives. And based to the comparison of protocols in the context of denaturation success, the fact that the additional bands had lower molecular weights than the expected CIP2A band, and that a single band representing human β-actin protein in each TNBC cell line appeared, supports the claim about protein degradation, rather than poor denaturation of proteins.

There is also a possibility that this non-specific labelling dues to the performance of anti-CIP2A. As written in the introduction, poor quality of commercial antibodies often causes problems in reproducibility. I also experienced difficulties in reproducing the results considering anti-CIP2A both during genetic validation and expression studies. Although I used the same sample conditions, and protocols through the studies, in addition to non-specific labelling, I also had problems with exposure times when visualizing the bands. For example, it is possible that the band representing TNBC cell line HCC70 in Figure 7c is overexposed. This could have impacted the visualization of other bands on this particular membrane. Due to these difficulties, I had to repeat CIP2A assays several times which led to waste of samples, antibodies, and other reagents. According to Trier et al. (2019) polyclonal antibodies have a higher risk for cross-reactivity than monoclonal products. But as the anti-CIP2A product used in this thesis is a monoclonal antibody, the clonality does not explain the problems in anti-CIP2A performance.

According to standard antibody validation criteria in western blot by The Human Protein Atlas (2022), the performance of the antibody is supported when the bands appear similar to the predicted molecular size in kDa (+/-20%), also when additional bands are present. Considering this, I conclude that while anti-CIP2A fulfilled the genetic validation criteria and its application was also supported based to this standard validation criterion in this given

western blot assay against human CIP2A, the performance of this antibody was not as good as the performance of anti-PME-1 or anti-SET.

4.1.2 Performance of anti-PME-1

On the membrane representing the genetic validation of anti-PME-1 (Figure 6b), I detected a single band corresponding to expected molecular weight of human PME-1, ~ 42–44 kDa. According to the reviewed UniprotKB entry Q9Y570 (2024b), PME-1 have two isoforms of this size, and other two sized ~ 18–22 kDa. The labelling of β-actin protein was not reduced after KD, as expected. I cannot compare my result to manufacturers product data as on this day, this given anti-PME-1 product is replaced with another product.

When I examined the western blot against human PME-1 with 18 TNBC samples (Figure 8c) in context of antibody performance, the target bands appeared corresponding to this ~ 44 kDa size. I also observed light additional bands, for example in sample lanes representing TNBC cell lines MDA-MB-468 and CAL120. The additional bands appeared both with higher and lower molecular weight compared to the band corresponding to the expected PME-1 band. As these additional bands were not seen in the genetic validation assay, it is possible that these particular TNBC samples are not fully denaturized in this given assay. On the other hand, a single band representing human β-actin protein in each TNBC cell line appeared which indicates that the denaturation has been sufficient. The additional bands with lower molecular weights can also due because of protein degradation, which was discussed above in the context of the performance of CIP2A. All in all, the performance of the anti-PME-1 fulfilled both the genetic validation criteria and the standard antibody validation criteria, presented earlier, in this given western blot assay with TNBC cell lines.

4.1.3 Performance of anti-SET

When I validated anti-SET with genetic strategy, I detected three bands with different molecular weight from the control sample. All bands corresponded to the molecular weight of ≥ 35 kDa. According to the reviewed UniprotKB entry Q01105 (2024c), SET has four known protein isoforms sized ~ 31–33 kDa, due to alternative splicing. According to the manufacturer (Santa Cruz Biotechnology Inc., 2025c), the immunogen of this given antibody is raised against human SET amino acids 1–120. When I compared the sequence of the immunogen to amino acid sequences of these four SET isoforms with BLAST tool (NCBI), I detected that the immunogen sequence is corresponding with all these four isoform sequences

presented at UniprotKB entry Q01105 (2024c). Based to this information, and the fact that the labelling was reduced significantly after SET-KD treatment, these three bands could possibly present different isoforms of SET. The labelling of β-actin protein was not reduced after KD, as I expected. The product data provided by the manufacturer (Santa Cruz Biotechnology Inc., 2025c) includes near-infrared western blot analysis result, in where the single band corresponds to higher molecular weight, compared to my result.

I also examined the performance of anti-SET in western blot with 18 TNBC samples (Figure 9c) and observed three bands corresponding to the genetic validation result of anti-SET. I also detected light additional bands, for example in the sample lanes representing TNBC cell lines MDA-MB-468, CAL120, and MDA-MB-436. All additional bands had lower molecular weight than three bands expected to represent protein SET. As discussed earlier in the context of the performance of CIP2A and PME-1, the protein degradation could explain this. The bands representing human β-actin protein from TNBC cell lines appeared as consistent in each lane, as expected.

Based on the conclusions considering SET isoforms, to determine expression level for SET protein, I quantified each band row separately, and then calculated the mean area value. However, I found difficulties to quantify area values not only because the three target bands, but also faint additional bands appeared, as described above. The quantification was also difficult because the migration of TNBC samples was uneven in this assay. According to Mahmood & Yang (2012) the resistance in the electrophoresis system impacts to the sample migration. I used the electrophoresis conditions provided by my instructor, but it is possible that for example, the voltage has been too high or the running time too low, or both. These conditions might have affected the sample migration and for example the sample stacking in the beginning of the drive. The other possibility is that the gel is stretched when I have placed it to blotting system causing the uneven appearance of some bands. Because the difficulties in quantifying, further studies with independent biological repeats are needed to examine SET protein expression more reliably.

Based on the performance of the anti-SET both in genetic validation assay and also in this given western blot assay with TNBC cell lines, I conclude that the use of this commercial antibody against human protein SET is supported.

4.2 PP2A inhibitor expression

The other aim of my thesis was to study the expression of PP2A inhibitor proteins CIP2A, PME-1 and SET across 18 human triple-negative breast cancer cell lines at mRNA level and protein level. I found no previous studies where these three PP2A inhibitor proteins would have been examined at the same time, so this question provided an interesting setting for research. Therefore, I was interested to study if one PP2A inhibitor would be distinguished from the other or if overlaps between PP2A inhibitors could be detected across TNBC cell lines and further among TNBC subtypes. Also, I found no articles considering PME-1 in the context of TNBC.

4.2.1 PP2A inhibitors overlap at mRNA level but at protein level CIP2A dominates over PME-1 and SET

Niemelä and colleagues (2012) have shown how the highest CIP2A mRNA expression levels can be associated with TNBC cell lines when compared to cell lines representing other breast cancer main types. Also, Liu and colleagues (2019) have earlier detected the overexpression of not only CIP2A but also SET mRNA in TNBC tissues. I also observed in my thesis, how all 18 TNBC cell lines overexpressed both CIP2A and SET at mRNA level, as was expected based on literature. I also found out that at protein level 15 TNBC cell lines out of 18 overexpressed CIP2A. This was also expected as in their immunohistochemical studies Niemelä et al. (2012) proved how high CIP2A protein levels were linked specifically to TNBC tumors. But interestingly, I also detected that only one TNBC cell line, the luminal AR MFM223 overexpressed SET at protein level. This cell line was also distinct as the only cell line overexpressing all three PP2A inhibitor proteins.

In the context of PME-1, I also noticed the difference between mRNA and protein expression across TNBC cell lines as nine cell lines out of 18 overexpressed PME-1 mRNA, but at protein level only four cell lines out of 18 overexpressed PME-1. Three out of these four cell lines also overexpressed CIP2A protein, except the mesenchymal-like cell line CAL120 which only overexpressed PME-1 protein.

So, half of the TNBC cell lines overexpressed all three PP2A inhibitors at mRNA level while, the other half overexpressed CIP2A and SET mRNAs. At protein level the trend was that only one PP2A inhibitor, mostly CIP2A, was overexpressed. Therefore, it can be stated that at mRNA level the overlapping between PP2A inhibitors is observed within the same TNBC

cell line but interestingly, at protein level CIP2A protein seems to dominate over PME-1 and SET proteins.

As TNBC tumors are known to form a heterogenous and complex group with lack of distinct targetable biomarkers, I was interested to examine the levels of overexpression of PP2A inhibitors within TNBC subtypes. I found out that at mRNA level both CIP2A and SET were overexpressed within all seven TNBC subtypes, which was expected since these two PP2A inhibitor mRNAs were overexpressed across all 18 cell lines. PME-1 mRNA was overexpressed within five subtypes. I also observed how the majority of TNBC subtypes overexpressed SET mRNA at the highest level of all three PP2A inhibitors. Only both mesenchymal origin subtypes overexpressed CIP2A mRNA with a higher level than SET mRNA. I also detected more variation between deviation values representing SET mRNA within each TNBC subtypes compared to other inhibitor mRNAs. This was also expected since, SET mRNA was overexpressed with a wider range across TNBC cell lines compared to CIP2A and PME-1 mRNAs.

However, within most of the subtypes SET and CIP2A mRNAs were overexpressed at quite similar levels. Two subtypes, the luminal AR and the immunomodulatory, differentiated from other subtypes as these overexpressed SET mRNA with distinctly higher levels than CIP2A mRNA. As presented in the result section, the SET mRNA expression level from the luminal AR subtype was the highest mean PP2A inhibitor mRNA level detected while, SET mRNA level from the single immunomodulatory cell line was the second highest. Within subtypes overexpressing all three inhibitor mRNAs, PME-1 mRNA was overexpressed at the lowest level compared to CIP2A and SET mRNAs.

As expected, based on expression results across TNBC cell lines, I observed that at protein level CIP2A was overexpressed within all seven TNBC subtypes while SET protein was overexpressed only in the luminal AR subtype. PME-1 protein was overexpressed within two subtypes, the luminal AR and the immunomodulatory, but only with a slightly high level.

And interestingly, not only CIP2A was the only inhibitor protein overexpressed within every subtype, but it was also expressed with distinctly higher levels than other PP2A inhibitors within most of the TNBC subtypes. Also, the deviation values representing CIP2A protein varied more across TNBC subtypes when compared to deviation values of PME-1 and SET proteins within each subtype. This was expected as CIP2A was expressed with a much wider

range across cell lines. Again, the luminal AR subtype was an exception as within this subtype all three inhibitors were overexpressed at quite similar levels.

Therefore, also across TNBC subtypes the domination of CIP2A protein over other PP2A inhibitor proteins can be detected while, at mRNA level, PP2A inhibitors seem to overlap. And, while both CIP2A and SET were overexpressed at mRNA level across all TNBC cell lines and thus across all TNBC subtypes, SET mRNA expression varied more than CIP2A. In comparison, at protein level only CIP2A was overexpressed in the majority of TNBC cell lines and within every TNBC subtype. CIP2A protein was also overexpressed with a wider range while, PME-1 and SET proteins were overexpressed with levels more even.

4.2.2 PP2A inhibitor expression variates within TNBC subtypes and among subtypes of the same origin

Based on the known heterogeneity of TNBC tumors and the variation I observed earlier, I was also interested to study PP2A inhibitors more specifically within each TNBC subtype. I detected variation within TNBC subtypes both at mRNA and protein level. Within the luminal AR subtype SET mRNA was overexpressed with a particularly high deviation as the overexpression levels of SET mRNA ranged from 2.9-fold to 7.6-fold. I also observed a great deviation in CIP2A protein expression within the mesenchymal stem-like and the basal-like 2 subtype. Within the mesenchymal stem-like subtype CIP2A protein overexpression levels ranged from 5.2- to 16.0-fold. And interestingly, within the basal-like subtype 2 three cell lines overexpressed CIP2A protein at from two- to almost eight-fold level while one cell line expressed CIP2A protein at 0.1-fold level.

I also wanted to study if TNBC subtypes with same origin share a similar expression pattern. I found out that at protein level there was variation between same origin subtypes as the mesenchymal stem-like subtype differentiates not only from other subtypes but also from the mesenchymal-like subtype. I detected that the CIP2A protein was overexpressed at 10-fold level within the mesenchymal stem-like subtype, while the expression of other PP2A inhibitors was not elevated. The mesenchymal-like subtype overexpressed CIP2A protein at 2.7-fold level, which was more similar to CIP2A levels within both basal origin subtypes. But this variation considered only CIP2A protein as, PME-1 and SET proteins were not overexpressed within the mesenchymal origin subtypes.

When I examined the basal origin subtypes, I detected that the basal-like 2 subtype overexpressed CIP2A protein more than the basal-like 1 but, the difference in overexpression levels was not as great as within mesenchymal origin subtypes. SET protein was expressed at similar level within both basal origin subtypes which was also similar to mesenchymal origin subtypes. The basal-like 1 expressed PME-1 protein a slightly more than the basal-like 2 but, as earlier mentioned, not as overexpressed.

I detected that at mRNA level TNBC subtypes of same origin shared more similar expression patterns. Both basal-like subtypes overexpressed SET mRNA at the highest level, CIP2A at the second highest, and PME-1 at the lowest. Both mesenchymal origin subtypes overexpressed CIP2A mRNA at the highest level while SET mRNA level was the second highest. Only the mesenchymal-like subtype overexpressed PME-1 mRNA but only at a slightly higher level compared to PME-1 expression in non-tumorigenic cell line MCF10A. As earlier detected in the context of mRNA expression across all subtypes, no great difference between CIP2A and SET mRNA expression levels between subtypes with same origin was observed.

Therefore, it can be stated that at mRNA level TNBC subtypes with same origin share a quite similar expression pattern but at protein level there was more variation in the context of CIP2A protein.

4.2.3 Correlation between mRNA and protein expression of PP2A inhibitor across TNBC cell lines

When I tested CIP2A protein as a function of CIP2A mRNA, I detected no correlation which was expected as CIP2A protein was expressed with a wide range across TNBC cell lines and with a high deviation within some TNBC subtypes. Also, there was no clear pattern between expression levels of CIP2A mRNA and CIP2A protein, as within half of the cell lines CIP2A protein level was lower than CIP2A mRNA level and within the other half CIP2A protein level was higher. For example, the basal like 2 cell line HCC1806 with the highest CIP2A mRNA level expressed CIP2A protein at six times lower level compared to the highest CIP2A protein expression, quantified from the mesenchymal stem-like cell line MDA-MB-231. In fact, the TNBC cell lines representing the mesenchymal stem-like subtype, had the lowest mean CIP2A mRNA expression but the highest mean CIP2A protein expression. Also, even while MDA-MB-231 cell line had the highest CIP2A protein level, it expressed CIP2A mRNA at 1.5 times lower level than the HCC1806 cell line, which had the highest CIP2A

mRNA expression. Therefore, a weak negative coefficient of correlation (r) was also expected.

When I tested PME-1 protein as a function of PME-1 mRNA, I observed a weak correlation. Also, in the context of SET protein versus SET mRNA, I detected a weak correlation. While the highest PME-1 mRNA level was five-fold compared to the lowest PME-1 mRNA level, the highest SET mRNA level was seven-fold compared to the lowest SET mRNA value. At protein level the highest PME-1 protein level was 15-fold compared to the lowest PME-1 protein expression value and, the highest SET protein value was 19-fold compared to the lowest SET protein value. In comparison, the highest CIP2A mRNA expression level was three-fold compared to the lowest CIP2A mRNA value but, the highest CIP2A protein value was almost 115-fold compared to the lowest CIP2A protein level. Therefore, these correlation findings were expected both PME-1 and SET were expressed with quite similar range both at mRNA and protein level while the range representing CIP2A was much wider.

Based on poor coefficient of determination values (R^2) in every correlation test, it can be stated that in this thesis mRNA levels do not explain much of the protein levels. Based to my findings, all PP2A inhibitors were overexpressed at mRNA level in the majority of TNBC cell lines but at protein level only CIP2A levels were elevated. So, the role of biological variables, such as post-transcriptionally and post-translationally regulation of PP2A inhibitors can be discussed. On the other hand, the fact that inhibitor mRNA expression values were referenced to the expression values in the non-tumorigenic cell line MCF10A, but protein expression levels were quantified in comparison of β-actin protein, means that mRNA and protein expressions cannot be fully compared with reliable way. I will discuss more about this when evaluating the reliability of this thesis in the chapter 4.3.

4.2.4 Correlation between PP2A inhibitors across TNBC cell lines at mRNA and protein level

Since I detected a similar expression pattern among PME-1 and SET both at mRNA and protein level, I was interested to study if there is a correlation between each PP2A inhibitor pair across TNBC cells at mRNA or protein level. I detected a significant correlation between PME-1 protein and SET protein and based on this finding, these two PP2A inhibitor proteins can be found overlapping across 18 TNBC cell lines. This was expected based on the fact, how similar the protein expression levels ranged across 18 TNBC cell lines between PME-1

and SET. Although PME-1 and SET proteins seem to overlap, it is important to remind that in the majority of TNBC cell lines neither of these PP2A inhibitors were overexpressed.

The positive correlation at mRNA level between SET and CIP2A have previously detected by Liu et al. (2019). Contrary to this expectation, I detected no correlation between CIP2A and SET, and further no between CIP2A and PME-1. Based on my findings in this thesis, this was expected since I found out that CIP2A was expressed with a much wider range and without a clear expression pattern across TNBC cell lines.

4.3 Reliability of thesis

The data considering the expression of PP2A inhibitors at mRNA level is reliable because the validity of primers was tested as prescribed in the methodological chapter 2.6. I also found no traces about the contamination in RT-qPCR. The preparation of master mix and adding the cDNA template for each reaction were done in separate environments. The reagents used for master mix were no contaminated as no signal from blank wells were detected, as expected. I also detected no high deviation between triplicates nor inconsistency between template amounts when pipetting and therefore, for example the sample mix up seems unlikely.

After each RT-qPCR run I detected only single Tm peaks, so no homo- or heterodimerization nor hairpin structures of primers occurred. I used blank controls, endogenous controls (*ACTB*) and samples as triplicates to produce technical repeats however, no independent biological repeats were used in this thesis, so no statistical tests were able to perform.

As the performance of the commercial antibodies was validated as trustworthy, based on the validation criteria used in this thesis, the original area data gathered from western blot studies can be found reliable. Because of the unsuccessful attempt to lyse the original protein pellets, mentioned in the chapter 2.3 and therefore, the lack of protein samples presenting the non-tumorigenic cell line MCF10A, the band areas of target protein were referenced to the band areas of β-actin protein. For that reason, the non-tumorigenic reference lacks and the values representing mRNA and protein expression levels cannot be fully compared. For reliable comparation, the β-actin protein level within MCF10A would have been needed to normalize the TNBC derived data against this non-tumorigenic cell line.

Also, the reliability of β-actin as an endogenous control can also be discussed. Even though this highly conserved structural protein is widely used as a reference to quantify expression

levels, it is known that altered β-actin expression is linked to cancer metastasis (Guo et al., 2013). Also, both of the mesenchymal origin TNBC subtypes examined in this thesis are known to be enriched with genes linked to cell motility (Lehmann et al., 2011). And for example, in mesenchymal stem-like MDA-MB-231 cells β-actin downregulation was linked to chromosomal instability (Dugina et al., 2021). Given this, for further research considering TNBC, known to be an invasive breast cancer type, I would assess the endogenous reference more carefully.

I also noticed some issues considering β-actin protein as a reference in western blot. I quantified the highest CIP2A protein expression from the mesenchymal stem-like cell line MDA-MB-231 (Figure 7b), But surprisingly, in western blot against human CIP2A (Figure 7c) I detected higher signals, and thus higher CIP2A expressions from samples representing TNBC cell lines Hs578T, BT549, MDA-MB-436, and HCC70. As I described in the methodological section (chapter 2.8), I quantified protein expression levels based on band area data with Fiji and, in the original area data these five cell lines: Hs578T, BT549, MDA-MB-231, MDA-MB-436, and HCC70 have higher values representing CIP2A band areas compared to other 13 cell lines. In the original area data MDA-MB-231 has the highest band area value for CIP2A but the lowest area value representing β-actin protein of all 18 TNBC cell lines. The other four cell lines in this example share similar and higher β-actin area values which clarifies the inconsistency when comparing band appearing in western blot membrane to quantified protein expression levels. Based on findings by Dugina et al. (2021) this low expression of β-actin in MDA-MB-231 cells is expected although, I have no data considering β-actin protein level in non-tumorigenic cell line MCF10A.

In retrospect, I would plan some of my laboratory work with a different way. For example, to ease the handling of data, I would load the TNBC samples for RT-qPCR and western blot according to TNBC subtypes. I would also test different protein extraction methods to prevent the precipitation and the potential waste of samples.

To gather more comprehensive data about the expression of PP2A inhibitors within and between different TNBC subtypes larger and equal amount of cell lines within each subtype would be needed. For example, I had only one cell line representing the immunomodulatory subtype. Also, to produce more scientifically reliable data, further research with independent biological repeats is needed.

4.4 Conclusions

Based on the validation criteria used in this thesis, all three commercial antibodies, anti-CIP2A, anti-PME-1, and anti-SET against PP2A inhibitors CIP2A, PME-1 and SET, respectively, are trustworthy to use. However, based on experienced difficulties in reproducing the experiments with anti-CIP2A product, more validation work would be needed to study other antibodies targeting human CIP2A and, to produce more reliable results and prevent the waste of resources in further studies. The results of the genetic validation studies of this thesis can be used when assessing the antibody candidates for further studies. However, as also this thesis shows, the antibodies must be validated for the assay planned to use, and the validation must be documented to indicate the reliability of the study.

As I already mentioned, I found no previous studies where CIP2A, PME-1 and SET would have been examined at the same time. In this thesis I show how three PP2A inhibitors overlap at mRNA level but at protein level CIP2A dominates over PME-1 and SET as, only CIP2A protein is overexpressed in majority of TNBC cell lines and within all seven TNBC subtypes. Therefore, this master thesis confirms the foreknowledge about the elevated levels of CIP2A protein in TNBC. This further means that because CIP2A overexpression, the crucial tumor suppressor protein PP2A is inhibited, and its targets, for example c-MYC and the oncogenic downstream effects of c-MYC remain in active state.

This thesis also confirms the foreknowledge about the elevated levels of SET mRNA in TNBC and also provides a new information considering the PME-1 expression in TNBC. I show how both PME-1 and SET are overexpressed in TNBC only at mRNA level but not at protein level hence, as active PP2A inhibitors. At protein level PME-1 and SET also overlapped, as these correlated significantly across TNBC cell lines. Therefore, based to this thesis, it seems that from these three PP2A inhibitor proteins, CIP2A is the most relevant in the context of TNBC. To examine the role of PME-1 in TNBC with more comprehensive way, both LCMT1, B-subunits of PP2A with different properties and also, the methylation status of C-subunit would be useful to include in further studies.

TNBC is already known to be a heterogenous breast cancer type and this thesis confirms this also from the perspective of CIP2A expression. I detected no clear expression pattern for CIP2A based on expression and correlation studies. At protein level CIP2A expression variates not only across 18 TNBC cell lines but also within subtypes and further between subtypes of same origin.

Interestingly, I detected how from seven TNBC subtypes especially, the mesenchymal stem-like subtype was distinct due to its ten-fold CIP2A protein level. The transcriptome of this subtype has earlier associated with cell growth and motility, and now also to elevated CIP2A protein level founded in this thesis. Based on this, the role of CIP2A protein overexpression as a potential clinical biomarker for this progressive mesenchymal stem-like TNBC is worth to be studied more closely. For example, could CIP2A be associated to anchorage-independent cell growth *in vitro* and tumor formation *in vivo* when cells representing the mesenchymal stem-like phenotype are studied.

I also found out that the luminal AR subtype was different as the only subtype overexpressing all three PP2A inhibitor proteins although, PME-1 was overexpressed only a slightly while SET level was similar with CIP2A level. So, while the overall trend is that CIP2A dominates over other inhibitor proteins, it seems that within the luminal AR TNBC subtype CIP2A, PME-1 and SET do overlap. However, more research with a larger amount of cell lines is needed to confirm this.

Acknowledgements

I would like to thank my supervisors Jukka Westermarck and Julia Vainonen from Westermarck lab. I am grateful for Jukka Westermarck for giving me the opportunity to join and learn in his team and providing me his professional guidance and, financial support. And thanks to Julia Vainonen for her guidance during the laboratory work. I would also like to thank all the members of Westermarck lab during the time I worked there for welcoming me and helping me when needed.

From the Department of Biology, I would like to thank my supervisor Päivi Koskinen for her expert guidance and support during this thesis project. I would also like to thank Sami Merilaita for giving his point of view and guidance during Tutkielmaryhmä gatherings.

And finally, I want to thank my family and friends. Especially thank you Rudy, for always being on my side, and Milla, thank you for your friendship with endless support.

References

Alfaleh, M. A., Alsaab, H. O., Mahmoud, A. B., Alkayyal, A. A., Jones, M. L., Mahler, S. M. & Hashem, A. M. (2020) Phage display derived monoclonal antibodies: From bench to bedside. Frontiers in Immunology 11, 1986.
DOI: 10.3389/fimmu.2020.01986

Baker, M. (2015) Reproducibility crisis: Blame it on the antibodies. Nature 521, 274–276.
DOI: https://doi.org/10.1038/521274a

Ballman, K. V. (2015) Biomarker: Predictive or prognostic? Journal of clinical oncology: official journal of the American Society of Clinical Oncology 33, 3968–3971.
DOI: https://doi.org/10.1200/JCO.2015.63.3651

Begley, C. G. & Ioannidis, J. P. A. (2015) Reproducibility in science: Improving the standard for basic and preclinical research. Circulation Research 116, 116–126.
DOI: https://doi.org/10.1161/CIRCRESAHA.114.303819

Bordeaux, J., Welsh, A., Agarwal, S., Killiam, E., Baquero, M., Hanna, J., Anagnostou, V. & Rimm, D. (2010) Antibody validation. BioTechniques 48, 197–209.
DOI: https://doi.org/10.2144/000113382

Chen, B., Hu, H. & Chen, X. (2023) From basic science to clinical practice: The role of cancerous inhibitor of protein phosphatase 2A (CIP2A)/p90 in cancer. Frontiers in Genetics 14, 1110656.
DOI: https://doi.org/10.3389/fgene.2023.1110656

Denkert, C., Liedtke, C., Tutt, A. & von Minckwitz, G. (2017) Molecular alterations in triple-negative breast cancer - the road to new treatment strategies. Lancet 389, 2430–2442.
DOI: https://doi.org/10.1016/S0140-6736(16)32454-0

Duffy, M. J., Harbeck, N., Nap, M., Molina, R., Nicolini, A., Senkus, E. & Cardoso, F. (2017) Clinical use of biomarkers in breast cancer: Updated guidelines from the European Group on Tumor Markers (EGTM). European Journal of Cancer 75, 284–298.
DOI: https://doi.org/10.1016/j.ejca.2017.01.017

Dugina, V., Shagieva, G., Novikova, M., Lavrushkina, S., Sokova, O., Kireev, I., & Kopnin, P. (2021) Impaired Expression of Cytoplasmic Actins Leads to Chromosomal Instability of MDA-MB-231 Basal-Like Mammary Gland Cancer Cell Line. Molecules 26, 2151.
DOI: https://doi.org/10.3390/molecules26082151

Eichhorn, P. J., Creyghton, M. P. & Bernards, R. (2009) Protein phosphatase 2A regulatory subunits and cancer. Biochimica et biophysica acta 1795, 1–15.
DOI: https://doi.org/10.1016/j.bbcan.2008.05.005

FDA-NIH Biomarker Working group (2016) Diagnostic Biomarker. BEST (Biomarkers, EndpointS, and other Tools) Resource. Silver Spring, MD; Bethesda, MD. US Food and Drug Administration; US National Institutes of Health.
Retrieved [9.2.2023] from https://www.ncbi.nlm.nih.gov/books/NBK402285/

Finnish Breast Cancer Group (2024) Rintasyövän valtakunnallinen diagnostiikka- ja hoitosuositus 2024. Levinneen rintasyövän hoito. Kolmoisnegatiivinen rintasyöpä, pp. 100.
Retrieved [7.9.2024] from https://rintasyoparyhma.yhdistysavain.fi/hoitosuositus/

Forsström, B., Axnäs, B. B., Rockberg, J., Danielsson, H., Bohlin, A. & Uhlen, M. (2015) Dissecting antibodies with regards to linear and conformational epitopes. PloS one 10, e0121673.
DOI: https://doi.org/10.1371/journal.pone.0121673

Foulkes, W. D., Smith, I. E. & Reis-Filho, J. S. (2010) Triple-negative breast cancer. The New England Journal of Medicine 363, 1938–1948.
DOI: https://doi.org/10.1056/NEJMra1001389

Frohner, I. E., Mudrak, I., Kronlachner, S., Schüchner, S. & Ogris, E. (2020) Antibodies recognizing the C terminus of PP2A catalytic subunit are unsuitable for evaluating PP2A activity and holoenzyme composition. Science signaling 13, eaax6490.
DOI: https://doi.org/10.1126/scisignal.aax6490

Garnock-Jones, K. P., Keating, G. M. & Scott, L. J. (2010) Trastuzumab: A review of its use as adjuvant treatment in human epidermal growth factor receptor 2 (HER2)-positive early breast cancer. Drugs 70, 215–239.
DOI: https://doi.org/10.2165/11203700-000000000-00000

Goossens, N., Nakagawa, S., Sun, X. & Hoshida, Y. (2015) Cancer biomarker discovery and validation. Translational Cancer Research 4, 256–269.
DOI: http://dx.doi.org/10.3978/j.issn.2218-676X.2015.06.04

Guo, C., Liu, S., Wang, J., Sun, M. Z. & Greenaway, F. T. (2013) ACTB in cancer. Clinica chimica acta; international journal of clinical chemistry 417, 39–44.
DOI: https://doi.org/10.1016/j.cca.2012.12.012

Henry, N. L. & Hayes, D. F. (2012) Cancer biomarkers. Molecular oncology 6, 140–146.
DOI: https://doi.org/10.1016/j.molonc.2012.01.010

Integrated DNA Technologies, Inc. (2024) OligoAnalyzerTM Tool. Applied [12.7.2021] in https://eu.idtdna.com/pages/tools/oligoanalyzer?returnurl=%2Fcalc%2Fanalyzer

International Agency for Research on Cancer (2024) Cancer today, Dataviz, Incidence and Mortality, Global Cancer Observatory. World Health Organization. Retrieved [18.3.2025] from https://gco.iarc.who.int/today/en/dataviz

Junttila, M. R., Puustinen, P., Niemelä, M., Ahola, R., Arnold, H., Böttzauw, T., Ala-aho, R., Nielsen, C., Ivaska, J., Taya, Y., Lu, S.-L., Lin, S., Chan, E. K. L., Wang, X.-J., Grènman, R., Kast, J., Kallunki, T., Sears, R., Kähäri, V.-M., Westermarck, J. (2007) CIP2A inhibits PP2A in human malignacies. Cell 130, 51–62. DOI: https://doi.org/10.1016/j.cell.2007.04.044

Kauko, O. & Westermarck, J. (2018) Non-genomic mechanisms of protein phosphatase 2A (PP2A) regulation in cancer. The International Journal of Biochemistry & Cell Biology 96, 157–164. DOI: https://doi.org/10.1016/j.biocel.2018.01.005

Kaur, A., Elzagheid, A., Birkman, E.-M., Avoranta, T., Kytölä, V., Korkeila, E., Syrjänen K., Westermarck, J. & Sundström, J. (2015) Protein phosphatase methylesterase-1 (PME-1) expression predicts a favorable clinical outcome in colorectal cancer. Cancer Medicine 4, 1798–1808. DOI: 10.1002/cam4.541

Kaur, A. & Westermarck, J. (2016) Regulation of protein phosphatase 2A (PP2A) tumor suppressor function by PME-1. Biochemical Society Transactions 44, 1683–1693. DOI: 10.1042/BST20160161

Khanna, A., Pimanda, J. E. & Westermarck, J. (2013) Cancerous inhibitor of protein phosphatase 2A, an emerging human oncoprotein and a potential cancer therapy target. Cancer Research 73, 1–6. DOI: 10.1158/0008-5472.CAN-13-1994

Laine, A., Nagelli, S. G., Farrington, C., Butt, U., Cvrljevic, A. N., Vainonen, J. P., Feringa, F. M., Grönroos, T. J., Gautam, P., Khan, S., Sihto, H., Qiao, X., Pavic, K., Connolly, D. C., Kronqvist, P., Elo, L. L., Maurer, J., Wennerberg, K., Medema, R. H., Joensuu, H., Peuhu, E., de Visser, K., Narla, G. & Westermarck, J. (2021) CIP2A interacts with TopBP1 and drives basal-like breast cancer tumorigenesis. Cancer Research 81, 4319–4331. DOI: 10.1158/0008-5472.CAN-20-3651

Laine, A., Sihto, H., Come, C., Rosenfeldt, M. T., Zwolinska, A., Niemelä, M., Khanna, A., Chan, E. K., Kähäri, V.-M., Kellokumpu-Lehtinen, P.-L., Sansom, O. J., Evan, G. I., Junttila, M. R., Ryan, K. M., Marine, J.-C., Joensuu, H. & Westermarck, J. (2013) Senescence sensitivity of breast cancer cells is defined by positive feedback loop between CIP2A and E2F1. Cancer Discovery 3, 182–197.
DOI: https://doi.org/10.1158/2159-8290.CD-12-0292

Lehmann, B. D., Bauer, J. A., Chen, X., Sanders, M. E., Chakravarthy, A. B., Shyr, Y. & Pietenpol, J. A. (2011) Identification of human triple-negative breast cancer subtypes and preclinical models for selection of targeted therapies. The Journal of Clinical Investigation 121, 2750–2767.
DOI: https://doi.org/10.1172/JCI45014

Leonard, D., Huang, W., Izadmehr, S., O'Connor, C. M., Wiredja, D. D., Wang, Z., Zaware, N., Chen, Y., Schlatzer, D. M., Kiselar, J., Vasireddi, N., Schüchner, S., Perl, A. L., Galsky, M. D., Xu, W., Brautigan, D. L., Ogris, E., Taylor, D. J. & Narla, G. (2020) Selective PP2A enhancement through biased heterotrimer stabilization. Cell 181, 688–701.
DOI: https://doi.org/10.1016/j.cell.2020.03.038

Li, J., Han, S., Qian, Z., Su, X., Fan, S., Fu, J., Liu, Y., Yin, X., Gao, Z., Zhang, J., Yu, D. & Ji, Q. (2014) Genetic amplification of PPME1 in gastric and lung cancer and its potential as a novel therapeutic target. Cancer Biology & Therapy 15, 128–134.
DOI: 10.4161/cbt.27146

Liu, C. Y., Huang, T. T., Chen, Y. T., Chen, J. L., Chu, P. Y., Huang, C. T., Wang, W. L., Lau, K. Y., Dai, M. S., Shiau, C. W. & Tseng, L. M. (2019) Targeting SET to restore PP2A activity disrupts an oncogenic CIP2A-feedforward loop and impairs triple negative breast cancer progression. EBioMedicine 40, 263–275.
DOI: https://doi.org/10.1016/j.ebiom.2018.12.032

Liu, Y., He, P., Zhang, M., Shi, L., Zhu, H., Wang, Z. & Zhao, J. (2013) Silencing of the human SET gene in vitro with lentivirus-mediated RNA interference. Molecular Medicine Reports 7, 843-847.
DOI: 10.3892/mmr.2013.1275

Livasy, C. A. (2017) Pathological evaluation of triple-negative breast cancer. Triple-Negative Breast Cancer. A Clinician's Guide 1–22.
DOI: 10.1007/978-3-319-69980-6_1

Longin, S., Zwaenepoel, K., Martens, E., Louis, J. V., Rondelez, E., Goris, J. & Janssens, V. (2008) Spatial control of protein phosphatase 2A (de)methylation. Experimental cell research 314, 68–81.
DOI: 10.1016/j.yexcr.2007.07.030

Mahmood, T. & Yang, P.-C. (2012) Western Blot: technique, theory, and trouble shooting. North American journal of medical sciences 4, 429–434.
DOI: 10.4103/1947-2714.100998

Mittendorf, E. A., Philips, A. V., Meric-Bernstam, F., Qiao, N., Wu, Y., Harrington, S., Su, X., Wang, Y., Gonzalez-Angulo, A. M., Akcakanat, A., Chawla, A., Curran, M., Hwu, P., Sharma, P., Litton, J. K., Molldrem, J. J. & Alatrash, G. (2014) PD-L1 expression in triple-negative breast cancer. Cancer immunology research 2, 361–370.
DOI: https://doi.org/10.1158/2326-6066.CIR-13-0127

Murphy, K. & Weaver, C. (2017) Antigen recognition by B-cell and T-cell receptors; Glossary. Janeway's Immunobiology. 9th edition. Garland Science, NY & London. pp. 139–152, 820.
Retrieved [11.10.2022] from https://inmunologos.files.wordpress.com/2020/08/janeways-immunobiology-9th-ed_booksmedicos.org_.pdf

Mäkelä, E., Löyttyniemi, E., Salmenniemi, U., Kauko, O., Varila, T., Kairisto, V., Itälä-Remes, M. & Westermarck, J. (2019) Arpp19 promotes Myc and Cip2a expression and associates with patient relapse in acute myeloid leukemia. Cancers 11, 1774.
DOI: https://doi.org/10.3390/cancers11111774

Nagelli, S. & Westermarck, J. (2024) CIP2A coordinates phosphosignaling, mitosis and the DNA damage response. Trends in Cancer 10, 52–64.
DOI: https://doi.org/10.1016/j.trecan.2023.09.001

National Cancer Institute (2022) Biomarker. NCI Dictionary of Cancer Terms.
Retrieved [11.10.2022] from https://www.cancer.gov/publications/dictionaries/cancer-terms/def/biomarker?redirect=true

National Center for Biotechnology Information (NCBI). Basic Local Alignment Search Tool. Applied [14.9.2021] in https://blast.ncbi.nlm.nih.gov/Blast.cgi

Niemelä, M., Kauko, O., Sihto, H., Mpindi, J.-P., Nicorici, D., Pernilä, P., Kallioniemi, O.-P., Joensuu, H., Hautaniemi, S. & Westermarck, J. (2012) CIP2A signature reveals the

MYC dependency of CIP2A-regulated phenotypes and its clinical association with breast cancer subtypes. Oncogene 31, 4266-4278.
DOI: 10.1038/onc.2011.599

Rossi, C., Cicalini, I., Cufaro, M. C., Consalvo, A., Upadhyaya, P., Sala, G., Antonucci, I., Del Boccio, P., Stuppia, L. & De Laurenzi, V. (2022) Breast cancer in the era of integrating "Omics" approaches. Oncogenesis 11, 17.
DOI: doi.org/10.1038/s41389-022-00393-8

Santa Cruz Biotechnology Inc. (2025a) CIP2A Antibody (2G10-3B5): sc-80659.
Retrieved [15.10.2025] from https://www.scbt.com/p/cip2a-antibody-2g10-3b5

Santa Cruz Biotechnology Inc. (2025b) Protocols. 1. Western (Immuno-) Blotting.
Retrieved [15.10.2025] from https://www.scbt.com/resources/protocols

Santa Cruz Biotechnology Inc. (2025c) I2PP2A Antibody (F-9): sc-133138.
Retrieved [15.10.2025] from https://www.scbt.com/p/i2pp2a-antibody-f-9

Schneider, B. P., Winer, E. P., Foulkes, W. D., Garber, J., Perou, C. M., Richardson, A., Sledge, G. W. & Carey, L. A. (2008) Triple-negative breast cancer: risk factors to potential targets. Clinical cancer research: an official journal of the American Association for Cancer Research 14, 8010–8018.
DOI: https://doi.org/10.1158/1078-0432.CCR-08-1208

Schroeder, H. W., Jr & Cavacini, L. (2010) Structure and function of immunoglobulins. The Journal of allergy and clinical immunology 125, Suppl 2, S41–S52.
DOI: https://doi.org/10.1016/j.jaci.2009.09.046

The Cancer Genome Atlas Network (2012) Comprehensive molecular portraits of human breast tumours. Nature 490, 61–70.
DOI: https://doi.org/10.1038/nature11412

The Human Protein Atlas (2022) Antibody validation.
Retrieved [20.9.2023] from https://www.proteinatlas.org/about/antibody+validation

Tozuka, K., Wongsirisin, P., Nagai, S. E., Kobayashi, Y., Kanno, M., Kubo, K., Takai, K., Inoue, K., Matsumoto, H., Shimizu, Y. & Suganuma, M. (2021) Deregulation of protein phosphatase 2A inhibitor SET is associated with malignant progression in breast cancer. Scientific Reports 11, 14238.
DOI: https://doi.org/10.1038/s41598-021-93620-y

Trier, N. H., Hansen, P. R. & Houen, G. (2012) Production and characterization of peptide antibodies. Methods 56, 136–144.
DOI: https://doi.org/10.1016/j.ymeth.2011.12.001

Trier, N. H., Hansen, P. R. & Houen, G. (2019) Peptides, antibodies, peptide antibodies and more. International Journal of Molecular Sciences 20, 6289. DOI: https://doi.org/10.3390/ijms20246289

Uhlén, M., Bandrowski, A., Carr, S., Edwards, A., Ellenberg, J., Lundberg, E., Rimm, D. L., Rodriquez, H., Hiltke, T., Snyder, M. & Yamamoto, T. (2016) A proposal for validation of antibodies. Nature Methods 13, 823–827. DOI: 10.1038/nmeth.3995

UniProtKB: the Universal Protein Knowledgebase (2024a) Q8TCG1; CIP2A_HUMAN. UniProt consortium. Retrieved [24.4.2024] from https://www.uniprot.org/uniprotkb/Q8TCG1/entry

UniProtKB: the Universal Protein Knowledgebase (2024b) Q9Y570; PPME1_HUMAN. UniProt consortium. Retrieved [24.4.2024] from https://www.uniprot.org/uniprotkb/Q9Y570/entry

UniprotKB: the Universal Protein Knowledgebase (2024c) Q01105; SET_HUMAN. UniProt consortium. Retrieved [24.4.2024] from https://www.uniprot.org/uniprotkb/Q01105/entry

Wang, J., Okkeri, J., Pavic, K., Wang, Z., Kauko, O., Halonen, T., Sarek, G., Ojala, P. M., Rao, Z., Xu, W. & Westermarck, J. (2017) Oncoprotein CIP2A is stabilized via interaction with tumor suppressor PP2A/B56. EMBO reports 18, 437–450. DOI: https://doi.org/10.15252/embr.201642788

Weller, M.G. (2018) Ten basic rules of antibody validation. Analytical Chemistry Insights 13. DOI: 10.1177/1177390118757462

Westermarck J. (2018) Targeted therapies don't work for a reason; the neglected tumor suppressor phosphatase PP2A strikes back. The FEBS journal 285, 4139–4145. DOI: https://doi.org/10.1111/febs.14617

Westermarck, J. & Hahn, W. C. (2008) Multiple pathways regulated by the tumor suppressor PP2A in transformation. Trends in molecular medicine 14, 152–160. DOI: https://doi.org/10.1016/j.molmed.2008.02.001

Westermarck, J. & Neel, B. G. (2020) Piecing together a broken tumor suppressor phosphatase for cancer therapy. Cell 181, 514-517. DOI: https://doi.org/10.1016/j.cell.2020.04.005

Zhao, G., Zhang, H., Zhang, Y., Zhao, N., Mao, J., Shang, P., Gao, K., Meng, Y., Tao, Y., Wang, A., Chen, Z. & Guo, C (2023) Oncoprotein SET dynamically regulates cellular

stress response through nucleocytoplasmic transport in breast cancer. Cell Biology and Toxicology 39, 1795–1814.
DOI: https://doi.org/10.1007/s10565-022-09784-4

Appendices

Appendix 1 Cell lines and cell culture

Table A1. Human derived triple-negative breast cancer cell lines, and their transcriptomic subtype according to Lehmann et al. (2011)

Cell line	Species	Transcriptomic subtype	Source
Hs578T	human	Mesenchymal Stem-like	ATCC
MDA-MB-468	human	Basal-like 1	ATCC
CAL120	human	Mesenchymal-like	DSMZ
CAL851	human	Basal-like 2	DSMZ
BT549	human	Mesenchymal-like	ATCC
MFM223	human	Luminal AR	DSMZ
CAL51	human	Mesenchymal-like	DSMZ
MDA-MB-231	human	Mesenchymal Stem-like	ATCC
MDA-MB-436	human	Mesenchymal Stem-like	ATCC
CAL148	human	Luminal AR	DSMZ
HCC1395	human	Unclassified	ATCC
HDQ-P1	human	Basal-like 2	DSMZ
DU4475	human	Immunomodulatory	DSMZ
HCC38	human	Basal-like 1	ATCC
HCC70	human	Basal-like 2	ATCC
HCC1806	human	Basal-like 2	ATCC
HCC1937	human	Basal-like 1	ATCC
BT20	human	Unclassified	ATCC

Table A2. Cell culture conditions

Cell line	**Growth medium**
Hs578T	RPMI 1640 + 10 % FBS + 2mM Glutamine + Pen/strep
MDA-MB-468	RPMI 1640 + 5 % FBS + 2mM Glutamine + Pen/strep
CAL120	DMEM + 10 % FBS + Pen/strep
CAL851	DMEM + 10 % FBS + 2mM Glutamine + 1mM Sodium Pyruvate + Pen/strep
BT549	RPMI 1640 + 10 % FBS + 2mM Glutamine + Pen/strep
MFM223	DMEM + 10 % FBS + 2mM Glutamine + Pen/strep
CAL51	DMEM + 20 % FBS + Pen/strep
MDA-MB-231	DMEM + 10 % FBS + 10µg/ml Insulin + Pen/strep
MDA-MB-436	DMEM + 10 % FBS + 10µg/ml Insulin + Pen/strep
CAL148	DMEM + 20 % FBS + 2mM Glutamine + EGF 0,1µg/l+ Pen/strep
HCC1395	RPMI 1640 + 10 % FBS + 2mM Glutamine + Pen/strep
HDQ-P1	DMEM + 10 % FBS + Pen/strep
DU4475	RPMI 1640 + 20 % FBS + 2mM Glutamine + Pen/strep
HCC38	RPMI 1640 + 10 % FBS + 2mM Glutamine + Pen/strep
HCC70	RPMI 1640 + 10 % FBS + 2mM Glutamine + Pen/strep
HCC1806	RPMI 1640 + 10 % FBS + 2mM Glutamine + Pen/strep
HCC1937	RPMI 1640 +10 % FBS + 2mM Glutamine + Pen/strep
BT20	RPMI 1640 + 10 % FBS + 2mM Glutamine + Pen/strep

Appendix 2 Protocol for siRNA treatment

Table A3. Small interfering RNA (siRNA) protocol

		6-well 1 X	plate, d = 20 cm 10 X	
Mixture	**Reagent**	**Volume (µl)**	**Volume (µl)**	
A	Opti-MEM™ Oligofectamine™ total	16 2 18	160 20 180	Prepare separately Incubation: 5 min, RT
B	Opti-MEM™ siRNA/control total	179.5 0.5 180	1795 5 1800	Prepare separately Incubation: 5 min, RT

Transfection mixture A + B, A = 0.1 B	Incubation: 10 min, RT

Table A4. Small interfering RNA (siRNA) sequences

Target	**Treatment name**	**Sequence 5'-3'**	**Source**
-	control	CGUACGCGGAAUACUUCGA	JW lab
CIP2A	CIP2A	CUGUGGUUGUGUUUGCACU	JW lab
PME-1	PME-1	GGAAGUGAGUCUAUAAGCA	JW lab
SET	SET	AAUGCAGUGCCUCUUCAUC	JW lab

Appendix 3 Protein lysis

Table A5. RIPA buffer

Reagent	**Concentration**
Tris-HCl, pH = 7.5	50 mM
NaCl	150 mM
Deoxycholic acid	0.5 %
SDS	0.1 %
Nonidet P-40 substitute	1 %

Appendix 4 Western blot

Table A6. Primary antibodies used in western blot

Product name	Vendor/ Cat. no.	Dilution	Incubation	Host animal	Clonality
CIP2A (2G10-3B5)	SC/ sc-80659	1/1000	overnight, 4 ℃	mouse	monoclonal
PME-1 (H-226)	SC/ sc-20086	1/1000	overnight, 4 ℃	rabbit	polyclonal
I2PP2A Antibody (F-9)	SC/ sc-133138	1/1000	overnight, 4 ℃	mouse	monoclonal
β-actin (C4)	SC/ sc-47778	1/2500	overnight, 4 ℃	mouse	monoclonal

SC for Santa Cruz Biotechnology

Table A7. Secondary antibodies used in western blot

Product name	Vendor	Cat. nro	Dilution	Incubation
Polyclonal Goat Anti-Mouse Immunoglobulin HRP	Dako	P0447	1/5000	1 h, RT
Polyclonal Swine Anti-Rabbit Immunoglobulin HRP	Dako	P0399	1/5000	1 h, RT

Appendix 5 RT-qPCR

Table A8. cDNA synthesis protocol for one sample volume

Component	**Quantity or volume**
RNA	1 μg
RNAse-free H_2O	ad. 17 μl
random hexamers (500 μg/ml)	0.5 μl
End volume	17.5 μl

Component	**Volume (μl)**	**Final concentration**
MMLV Rtase buffer (5X)	5	1X
RNAsin (40 U/μl)	0.25	0.4 U
dNTP Mix (10 mM)	1.25	0.5 mM
MMLV Rtase (200 U/μl)	1	8 U
End volume	7.5	

Table A9. RT-qPCR reaction for one well volume

Reagent	**Volume (μl)**	
nuclease-free H2O	7	master mix
PowerUp™ SYBR™ Green Master Mix (2X) Cat. no. A25742, Applied Biosystems™	10	
primer mix (F + R, 5 μM each)	1	
cDNA	2	
end volume	20	

Table A10. RT-qPCR protocol

Phase	**Temperature (℃)**	**Time (s)**	
Initial denaturation	95	120	
Denaturation	95	15	40 cycles
Annealing	60	60	
Extension	60	60	

Table A11. RT-qPCR primers

Gene symbol (NCBI)	Sequence 5'–3'	Tm (℃)	Length	GC%	Source
ACTB	5'-CCAACCGCGAGAAGATGA-3'	60	18	56	JW lab
	5'-CCAGAGGCGTACAGGGATAG-3'	59	20	60	
CIP2A	5'-TCCACTGCCTGCTTGAAGTC-3'	57.5	20	55	JW lab
	5'-GAAATTACCTCCAAGTGCCGC-3'	56.6	21	52.4	
PPME1	5'-ACAGGTTTGCAGAACCCATC-3'	55.6	20	50	JW lab
	5'-GGACAGCAGGTCACTAACAGC-3'	57.9	21	57.1	
SET	5′-AAATATAACAAACTCCGCCAACC-3′	53.7	23	39.1	Liu, Y. et al. (2013)
	5′-CAGTGCCTCTTCATCTTCCTC-3′	55.1	21	52.4	